Title
Bromoform and dibromomethane measurements in the seacoast region of New Hampshire, 2002–2004

Journal
Journal of Geophysical Research, 113(D8)

ISSN
0148-0227

Authors
Zhou, Yong
Mao, Huiting
Russo, Rachel S
et al.

Publication Date
2008

DOI
10.1029/2007jd009103

Bromoform and dibromomethane measurements in the seacoast region of New Hampshire, 2002–2004

Yong Zhou,[1] Huiting Mao,[1] Rachel S. Russo,[1] Donald R. Blake,[2] Oliver W. Wingenter,[3] Karl B. Haase,[1,3] Jesse Ambrose,[1] Ruth K. Varner,[1] Robert Talbot,[1] and Barkley C. Sive[1]

Received 27 June 2007; revised 27 September 2007; accepted 19 December 2007; published 24 April 2008.

[1] Atmospheric measurements of bromoform ($CHBr_3$) and dibromomethane (CH_2Br_2) were conducted at two sites, Thompson Farm (TF) in Durham, New Hampshire (summer 2002–2004), and Appledore Island (AI), Maine (summer 2004). Elevated mixing ratios of $CHBr_3$ were frequently observed at both sites, with maxima of 37.9 parts per trillion by volume (pptv) and 47.4 pptv for TF and AI, respectively. Average mixing ratios of $CHBr_3$ and CH_2Br_2 at TF for all three summers ranged from 5.3–6.3 and 1.3–2.3 pptv, respectively. The average mixing ratios of both gases were higher at AI during 2004, consistent with AI's proximity to sources of these bromocarbons. Strong negative vertical gradients in the atmosphere corroborated local sources of these gases at the surface. At AI, $CHBr_3$ and CH_2Br_2 mixing ratios increased with wind speed via sea-to-air transfer from supersaturated coastal waters. Large enhancements of $CHBr_3$ and CH_2Br_2 were observed at both sites from 10 to 14 August 2004, coinciding with the passage of Tropical Storm Bonnie. During this period, fluxes of $CHBr_3$ and CH_2Br_2 were 52.4 ± 21.0 and 9.1 ± 3.1 nmol m^{-2} h^{-1}, respectively. The average fluxes of $CHBr_3$ and CH_2Br_2 during nonevent periods were 18.9 ± 12.3 and 2.6 ± 1.9 nmol m^{-2} h^{-1}, respectively. Additionally, $CHBr_3$ and CH_2Br_2 were used as marine tracers in case studies to (1) evaluate the impact of tropical storms on emissions and distributions of marine-derived gases in the coastal region and (2) characterize the transport of air masses during pollution episodes in the northeastern United States.

Citation: Zhou, Y., H. Mao, R. S. Russo, D. R. Blake, O. W. Wingenter, K. B. Haase, J. Ambrose, R. K. Varner, R. Talbot, and B. C. Sive (2008), Bromoform and dibromomethane measurements in the seacoast region of New Hampshire, 2002–2004, *J. Geophys. Res.*, *113*, D08305, doi:10.1029/2007JD009103.

1. Introduction

[2] Bromoform ($CHBr_3$) and dibromomethane (CH_2Br_2) are predominantly marine-derived brominated organic compounds and have much shorter atmospheric lifetimes than halons and methyl bromide (CH_3Br). Short-lived brominated organic compounds, such as $CHBr_3$ and CH_2Br_2, with lifetimes of ~2–3 weeks and ~2–3 months, respectively, have been identified as sources of the reactive radical species BrO_x (Br + BrO) to the atmosphere [*Carpenter and Liss*, 2000; *McGivern et al.*, 2000; *Quack and Wallace*, 2003]. Reactive bromine chemistry has been linked to surface ozone depletion in various regions, including the Arctic and Antarctica [*Foster et al.*, 2001; *Bottenheim et al.*, 2002], coastal areas [*Nagao et al.*, 1999; *Galbally et al.*, 2000] and the marine boundary layer [*Sander and Crutzen*, 1996; *von Glasow et al.*, 2002]. Under strong convective conditions, which predominantly occur in the tropics, $CHBr_3$ and CH_2Br_2 can be transported to the stratosphere, thus contributing to ozone depletion [*Dvortsov et al.*, 1999; *Schauffler et al.*, 1999; *Sturges et al.*, 2000; *Nielsen and Douglass*, 2001; *Montzka et al.*, 2003]. Previous observations and modeling studies suggest significant contributions (~30% to >60%) of $CHBr_3$ to inorganic Br levels within the upper troposphere and lower stratosphere [*Dvortsov et al.*, 1999; *Nielsen and Douglass*, 2001; *Quack and Wallace*, 2003]. The production, emission rates and atmospheric distributions of these short-lived gases are spatially and temporally variable. Uncertainties still exist in the short-lived organic bromine budget and its contribution to atmospheric bromine chemistry. Atmospheric observations of $CHBr_3$ and CH_2Br_2 in the northwest Atlantic coastal regions are limited in number [*Quack and Wallace*, 2003]. Moreover, climate change, such as global warming and the feedbacks associated with temperature changes, could influence regional and global macroalgae abundances and distributions, and thus the production of marine-derived

[1] Climate Change Research Center, Institute for the Study of Earth, Oceans, and Space, University of New Hampshire, Durham, New Hampshire, USA.
[2] Department of Chemistry, University of California, Irvine, California, USA.
[3] Department of Chemistry, New Mexico Tech, Socorro, New Mexico, USA.

0148-0227/08/2007JD009103

gases. Measurements of these gases provide valuable information on their regional and global distributions, budgets, and contributions to bromine chemistry in the troposphere. Although the primary mechanism for injection of these gases into the stratosphere occurs through convective activity in the tropics, measurements of these gases at a wide range of locations in the tropical oceans, as well as other regions, including midlatitude and high-latitude coastal zones, are fundamental in order to accurately estimate their global budgets for climate and modeling studies related to stratospheric ozone depletion. Furthermore, these gases have been frequently used as tracers to investigate the marine influence on air masses [e.g., *Atlas et al.*, 1992; *Blake et al.*, 1996a, 1999b; *Zhou et al.*, 2005]. Measurements of these marine tracers are important to improve our understanding of the atmospheric processes that control the production and distribution of air pollutants along coastal regions.

[3] Marine macro and microalgae produce $CHBr_3$ and CH_2Br_2 [*Gschwend et al.*, 1985; *Manley et al.*, 1992; *Sturges et al.*, 1992; *Moore and Tokarczyk*, 1993; *Carpenter and Liss*, 2000; *Quack and Wallace*, 2003]. Previously reported studies indicate much higher production rates and subsequent emissions of $CHBr_3$ in coastal regions compared to the open ocean [e.g., *Zhou et al.*, 2005]. Assessments of algal biomass and halocarbon emission estimates suggest that macroalgae in coastal regions contribute about 70% of the global atmospheric $CHBr_3$ production [*Carpenter and Liss*, 2000]. Meridional surveys over the eastern Atlantic and the western Pacific Oceans have revealed maximum levels in the tropical marine boundary layer resulting from enhanced regional biogenic production [*Quack and Wallace*, 2003]. Seasonal trends of the production rates and distributions for $CHBr_3$ and CH_2Br_2 are quite variable among different studies [*Carpenter and Liss*, 2000; *Quack and Wallace*, 2003]. The global emission estimate of CH_2Br_2 was estimated by *Carpenter et al.* [2003] to be ~15–25% of the global $CHBr_3$ flux, which is $\sim 2.2 \times 10^{11}$ g $CHBr_3$ yr^{-1} [*Carpenter and Liss*, 2000]. In some coastal regions, where numerous disinfection facilities and power plants dump effluent into coastal waters, chlorination of water may serve as an additional source of $CHBr_3$. In this process, hypochlorite and hypobromite react with organic material producing trihalomethanes (THMs) [*Fogelqvist and Krysell*, 1991; *Jenner et al.*, 1997; *Allonier et al.*, 1999; *Quack and Wallace*, 2003], with $CHBr_3$ as the principal by-product [*Allonier et al.*, 1999].

[4] Photolysis and reaction with hydroxyl radical (OH) are the main atmospheric sinks of $CHBr_3$, yielding a photochemical lifetime of ~2–3 weeks [*Carpenter and Liss*, 2000]. For CH_2Br_2, reaction with OH is the major removal mechanism with a lifetime of ~2–3 months [*Schauffler et al.*, 1999]. Median concentrations of these two gases measured in the tropical marine boundary layer from Transport and Chemical Evolution over the Pacific (TRACE-P) and Pacific Exploratory Mission in the Tropical Pacific (PEM-Tropics) A and B were 1.10–1.83 pptv for $CHBr_3$ and 1.07–1.33 pptv for CH_2Br_2 [*Blake et al.*, 1999a, 1999b, 2001, 2003]. Mean concentrations of $CHBr_3$ measured in the tropical marine boundary layer (10°–45°N) from Pacific Exploratory Mission in the Tropical Pacific (PEM-Tropics) A (late August to early October 1996) and B (March and early April 1999) were 0.58 and 0.85 pptv, respectively [*Blake et al.*, 2003]. A mean atmospheric mixing ratio of 0.5 pptv for $CHBr_3$ was observed in the open ocean of the northern Atlantic (0–66°N) in October 1996 [*Fischer et al.*, 2000]. However, its concentrations were significantly higher in coastal regions. Atmospheric mixing ratios of $CHBr_3$ measured at the coastal site Mace Head (53.3°N, 9.9°W), Ireland, ranged from 1.0 to 22.7 pptv, with a mean value of 6.3 and 6.8 pptv in May 1997 and September 1998, respectively [*Carpenter et al.*, 1999, 2003]. In air masses with recent marine influences, a positive correlation between $CHBr_3$ and CH_2Br_2 has been observed [*Carpenter et al.*, 2003; *Zhou et al.*, 2005]. Because in situ atmospheric sources of these two gases have never been previously reported, the positive correlation between them indicates that they have common sources and similar sinks.

[5] Measurements of key atmospheric species at Thompson Farm (TF) in Durham, NH, and Appledore Island (AI), ME, were conducted with the goal of addressing fundamental gaps in our knowledge of atmospherically relevant trace gas distributions, oxidative processing of anthropogenic and biogenic organic carbon species and the mechanisms of aerosol formation and aerosol modification. This paper focuses on the distributions of the oceanic short-lived brominated organic compounds, investigates the factors affecting their distributions and uses these gases as tracers to better understand the marine influences on regional air quality. Atmospheric mixing ratios of $CHBr_3$ and CH_2Br_2 were measured from 1 June to 31 August 2002, 3 July to 17 September 2003, and 2 July to 15 August 2004, at TF and from 2 July to 13 August 2004, at AI. Vertical profiles over the coastal region of the Gulf of Maine were obtained from measurements conducted aboard the NASA DC-8 aircraft as part of the Intercontinental Chemical Transport Experiment - North America (INTEX-NA) during the International Consortium for Atmospheric Research on Transport and Transformation (ICARTT) 2004 campaign, a joint research effort by scientists from North America and Europe. Atmospheric distributions of $CHBr_3$ and CH_2Br_2 are interpreted with local meteorology to investigate source region relationships. Correlations of $CHBr_3$ with CH_2Br_2 and $CH_2Br_2/CHBr_3$ with $CHBr_3$ are presented to illustrate their common sources and to study the evolution of the compositions of air masses for a coastal and inland site. Additionally, $CHBr_3$ and CH_2Br_2 are used as marine tracers in case studies to determine the impact of tropical storms and characterize the transport of air masses during pollution episodes in New England.

2. Observational Methods

2.1. Field Site Description

[6] The University of New Hampshire Observing Station at Thompson Farm (TF) (43.11°N, 70.95°W, elevation 24 m) is located in the southeastern, rural area of Durham, New Hampshire (Figure 1). Thompson Farm is 24 km from the Gulf of Maine and 5 km northwest of Great Bay, NH, and is located on an active corn farm surrounded by a mixed forest. Air is drawn down a PFA Teflon-lined manifold from the top of a 12-m tower. A subsample of this air is directed to our automated gas chromatographic

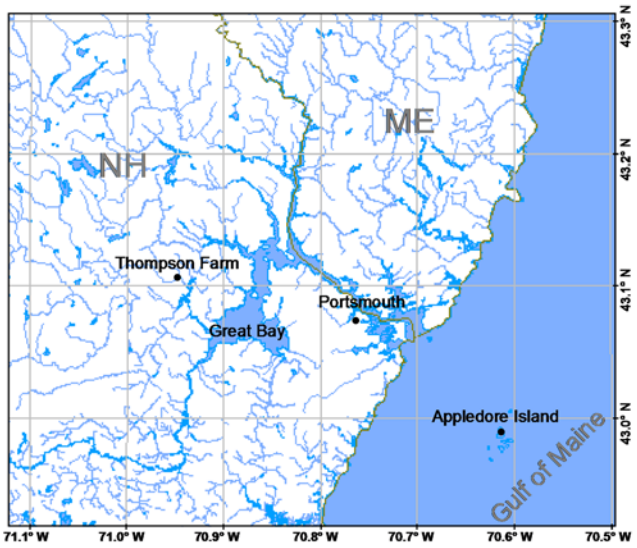

Figure 1. Locations for two of the AIRMAP monitoring stations: Thompson Farm in Durham, New Hampshire, and Appledore Island, Maine.

(GC) system equipped with two flame ionization detectors (FIDs) and two electron capture detectors (ECDs) for the analysis of hydrocarbons, halocarbons, and alkyl nitrates. The UNH Observing Station at Appledore Island (AI) is located at the Shoals Marine Lab on Appledore Island, ME (42.97°N, 70.62°W, sea level), which is part of the Isles of Shoals. Located off the coast of Maine and New Hampshire, AI is a unique sampling location, where air masses that have been influenced by a variety of different source regions, including coastal marine, the forested sub-Arctic, the industrialized Midwestern United States, the metropolitan East Coast and the open North Atlantic Ocean, are frequently encountered.

2.2. Analytical Methods

2.2.1. Thompson Farm GC System

[7] Details regarding the automated GC system deployed at Thompson Farm can be found in the work of *Zhou et al.* [2005], *Sive et al.* [2005], and *Zhou* [2006]. Current modifications of the system during the ICARTT campaign are described below. Briefly, the TF GC system is designed for dual stage trapping using liquid nitrogen such that there are two individual dewars containing cold regions – the first stage is for water removal and is cooled to −20°C, while the second stage is used for sample concentration and is cooled to −185°C. The first stage cooling unit contains an empty 6-inch × 1/8-inch Silonite-coated (Entech Instruments, Inc., Simi Valley, CA) stainless-steel sample loop while the second stage contains a 6-inch × 1/8-inch Silonite-coated stainless-steel sample loop filled with glass beads (60/80 mesh) for sample concentration. From studies conducted at TF, we have determined that −20°C is adequate for water removal during the sample trapping procedure, even during extremely high humidity episodes encountered during the summer months.

[8] Numerous experiments have been conducted to ensure that the trace gases of interest are not lost in the water removal loop and are recovered quantitatively. Table 1 shows the results of one such experiment illustrating quantitative recovery of CH_2Br_2 and $CHBr_3$ when varying the water removal loop temperature from −30°C to 30°C. At the 95% confidence level, there is no statistical difference in the peak areas obtained for the triplicate measurements using a humidified whole air standard, illustrating that the compounds of interest were not retained by the water removal loop.

[9] After the loops reached their initial set point temperatures, a downstream mass flow controller and pump were used to draw a 1200-cc aliquot from the sampling manifold at a rate of 200 cc min^{-1}. After sample trapping was complete, 100 cc of UHP helium was passed through both loops at a rate of 100 cc min^{-1}. After the helium sweep, the glass bead filled sample loop was isolated, rapidly heated (∼10 s) to 100°C, and then injected. Helium carrier gas flushed the contents of the loop and the stream was split into four, with each substream feeding a separate GC column housed in a single gas chromatograph. One 50 m × 0.53 mm I.D., 10-μm film thickness CP-$A1_2O_3/Na_2SO_4$ PLOT column (Varian, Inc., Walnut Creek, CA), one 60 m × 0.32 mm I.D., 1.0-μm film thickness VF-5ms column (Varian, Inc., Walnut Creek, CA), one 60 m × 0.25 mm I.D., 1-μm film thickness OV-1701 column (Ohio Valley, Marietta, OH), and one 25 m × 0.25 mm I.D., 3.0-μm film thickness CP-PoraBOND-Q (Varian, Inc., Walnut Creek, CA) coupled to a 40 m× 0.25 mm I.D., 0.5-μm film thickness OV-5 column (Ohio Valley, Marietta, OH) were used for trace gas separation (denoted as the PBQ-OV5). The OV-1701 and PBQ-OV5 columns were plumbed into the ECDs and used for quantifying halocarbons and alkyl nitrates. The PLOT and VF-5 ms columns were connected to the FIDs and used for the C_2-C_{10} nonmethane hydrocarbon (NMHC) measurements. Specifically, the OV-1701 ECD channel of the TF GC was used for quantifying CH_2Br_2 and $CHBr_3$.

[10] After the sample is injected, the water removal and sample concentration loops are both heated and backflushed with UHP helium for 5 min at 100°C during the bake-out period to ensure the loops are clean prior to cooling for concentration of the subsequent sample [*Sive et al.*, 2005]. For the standard analysis protocol, a 1200-cc aliquot from one of two working standards was assayed every ninth analysis, thereby quickly drawing attention to any drift or malfunction of the analytical system. During the ICARTT campaign, the time required for one complete cycle of trapping, injecting, and chromatographic separation was approximately 40 min.

2.2.2. Appledore Island Canister Samples

[11] Hourly samples were collected in 2-liter electropolished stainless steel canisters (University of California, Irvine (UCI)) at AI for C_2-C_{10} NMHCs, C_1-C_2 halocar-

Table 1. Compound Recovery Results for CH_2Br_2 and $CHBr_3$ When Varying the Water Management Loop Temperature of the TF GC[a]

Temperature, °C	CH_2Br_2	$CHBr_3$
−30	29622 ± 2073	13419 ± 1124
−20	34796 ± 2087	14653 ± 1026
0	31332 ± 2193	14377 ± 1150
30	33898 ± 2101	13828 ± 1037

[a]Values are expressed as average peak area ± standard deviation for triplicate analyses of a humidified whole air standard.

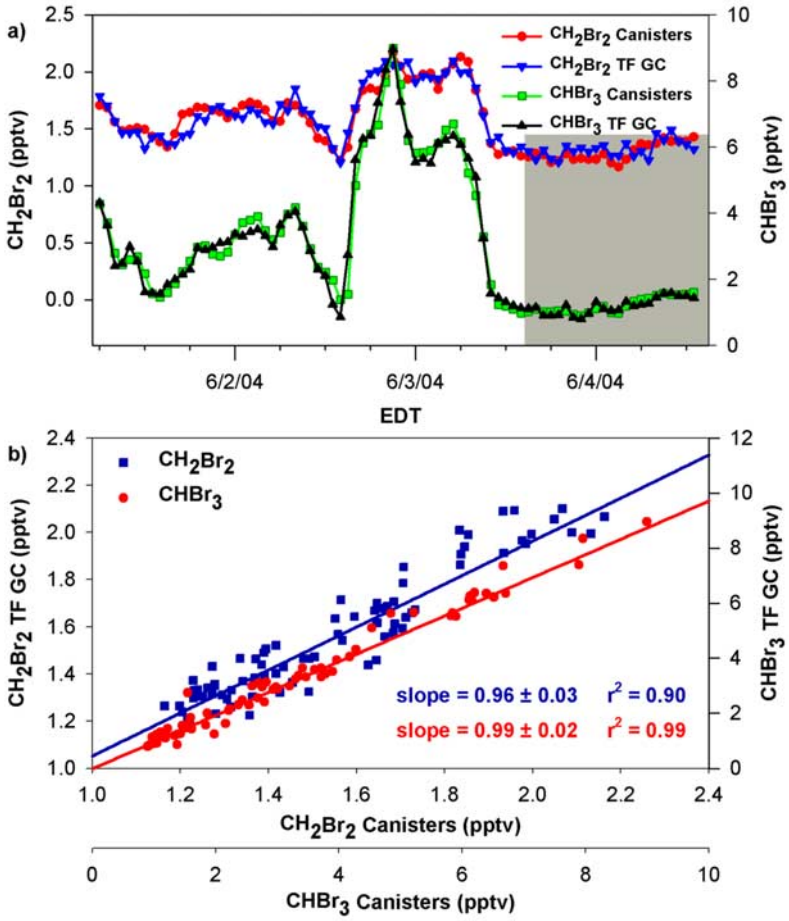

Figure 2. Measurements conducted at Thompson Farm (TF) from 1 to 4 June 2004 to compare quantitative results from the TF gas chromatographic (GC) with the canister system. (a) Time series plot of CH_2Br_2 and $CHBr_3$ for the TF GC and canister system. (b) Correlations of CH_2Br_2 and $CHBr_3$ for the canister system versus the TF GC. The gray shaded area in Figure 2a represents the time period used to estimate the measurement precision for each compound.

bons, C_1–C_5 alkyl nitrates and selected organic sulfur compounds from the top of a World War II-era lookout tower (~20 m), 2 July to 13 August 2004. Canister samples were pressurized to 35 psig using a single-head metal bellows pump (MB-302MOD, Senior Flexonics, Sharon, MA) and returned to our laboratory at UNH every 4 d for analysis by gas chromatography using a three GC system equipped with two ECDs, two FIDs and one mass spectrometer (MS). The samples were analyzed by cryotrapping 1772 cc (STP) of air on a glass bead filled loop immersed in liquid nitrogen. After the sample was trapped, the loop was isolated, warmed to 80°C and the sample was injected. Helium carrier gas flushed the contents of the loop and the stream was split into five, with each substream feeding a separate GC column. One 30 m × 0.53 mm I.D., 10-μm film thickness CP-$A1_2O_3/Na_2SO_4$ PLOT column, one 60 m × 0.25 mm I.D., 1-μm film thickness OV-1701 column, one 60 m × 0.32 mm I.D., 1.0-μm film thickness DB-1 column (J&W Scientific, Folsom, CA), and two 60 m × 0.25 mm I.D., 1.4-μm film thickness OV-624 columns (Ohio Valley, Marietta, OH) were used for the trace gas separation. One of the OV-624 columns and the OV-1701 column were plumbed into ECDs and used for measuring the halocarbons and alkyl nitrates. The PLOT and DB-1 columns were connected to FIDs and used for C_2–C_{10} NMHC quantification. The second OV-624 column provided separation for the MS. Electron impact mode for the MS was used for sample ionization along with single ion monitoring. This system provided duplicate measurements for numerous halocarbons and NMHCs. Finally, the gas separation was unique for each of the columns, and thus, any gases coeluting on one column were usually resolved on another. Similar to the TF GC system, the OV-1701 ECD channel of the canister system was used for quantifying CH_2Br_2 and $CHBr_3$. The standard analysis protocol was identical to that used at TF (section 2.2.1). The time required for one complete cycle of trapping, injecting, and chromatographic separation was approximately 30 min. Further details regarding the AI sample analysis can be found in the work of *Sive et al.* [2005], *Zhou et al.* [2005], and *Zhou* [2006].

2.2.3. Quantitative Analytical System Comparison

[12] Prior to the ICARTT summer campaign, a 4-d study was conducted from 1 to 4 June 2004 to ensure comparable quantitative results between the automated GC at TF and the canister samples to be collected at AI and returned to our laboratory for analysis. Hourly samples were collected in 2-liter electropolished stainless steel canisters (UCI) and pressurized to 35 psig using a single head metal bellows

Table 2. Measurement Precisions of CH_2Br_2 and $CHBr_3$ Based on the Analysis of Whole Air Standards During the ICARTT Campaign for the TF GC and the Canister System[a]

System	Standard	Count	CH_2Br_2, pptv	CH_2Br_2, %RSD	$CHBr_3$, pptv	$CHBr_3$, %RSD
TF GC	Std 0	66	0.69 ± 0.04	5.5	0.48 ± 0.04	7.5
TF GC	DC2	79	1.20 ± 0.06	4.9	0.61 ± 0.04	6.9
Canister	Pont2	130	0.81 ± 0.03	3.7	0.69 ± 0.03	3.6
Canister	CCR28	126	0.50 ± 0.02	4.8	0.30 ± 0.02	6.1

[a]Mixing ratios and standard deviations are expressed in pptv. %RSD is the percent relative standard deviation.

pump over the 4-d study period. As shown in Figure 2a for CH_2Br_2 and $CHBr_3$, a moderate sized event was captured during the study period which was flanked by episodes of clean air. This fortuitous phenomenon enabled us to roughly bracket low and high mixing ratios that were expected during the ICARTT campaign. Furthermore, Figure 2b shows the correlations of CH_2Br_2 and $CHBr_3$ for the TF GC and canister samples yielding the following results: CH_2Br_2 (slope = 0.96 ± 0.03, r^2 = 0.90), $CHBr_3$ (slope = 0.99 ± 0.02, r^2 = 0.99). The results from this study help illustrate that the measurements during the ICARTT campaign at TF and AI can be accurately compared.

[13] Additionally, an informal intercomparison experiment was conducted by D. Blake at UCI to evaluate the comparability of measurements between different investigators carrying out VOC measurements on various platforms during the ICARTT campaign. Each investigator was sent four pressurized canisters filled with whole air collected by the UCI group and was asked to analyze them for the suite of gases they were measuring during the campaign. Mixing ratios for each of the gases in the individual canisters as well as the average of the four samples were reported to D. Blake to evaluate the calibration scales between the participating research groups. The UNH group reported a total of 99 gases which included a suite of C_2–C_{10} NMHCs, C_1–C_5 alkyl nitrates, C_1–C_2 halocarbons and carbonyl sulfide. For the 52 gases included in the intercomparison experiment, the average percent difference between UCI and UNH was 6.1% (D. Blake, UCI, personal communication, 2005). The average mixing ratios reported by UNH for CH_2Br_2 and $CHBr_3$ were 1.60 ± 0.07 and 5.30 ± 0.19 pptv, respectively. At the 95% confidence level, the values reported by UNH agreed with the UCI mixing ratios of 1.45 ± 0.07 for CH_2Br_2 and 5.18 ± 0.10 pptv for $CHBr_3$.

2.2.4. Measurement Precision of CH_2Br_2 and $CHBr_3$

[14] To evaluate the overall measurement precision for CH_2Br_2 and $CHBr_3$, the working standard values were used to estimate the precision for each of the analytical systems employed during the ICARTT campaign. The primary working standards used for the TF GC system were two different pressurized whole air samples contained in Luxfer aluminum high-pressure gas cylinders (Scott Marin, Riverside, CA). For the canister analytical system, two calibrated whole air samples contained in 36-liter electropolished low-pressure pontoons (~350 psi) were used as the primary working standards. The low-pressure pontoons contained similar mixing ratios for the full suite of NMHCs, alkyl nitrates and halocarbons as the standards used for the TF GC. All gases in the whole air standards were previously calibrated using synthetic standards and other whole air standards for cross referencing the mixing ratios.

[15] During the course of the campaign, the working standards were analyzed after every ninth sample, alternating between each of the two standards. To monitor any drift in the standard or the analytical system, other pressurized whole air standards were also assayed throughout the project. Because of the relatively high frequency of standard analyses (4–6 h), it was possible to monitor small changes for each analytical system over the duration of the project.

[16] All standard and sample chromatograms were manually baseline checked after the analyses were complete to ensure all peaks were properly identified and integrated. The standards were then used to correct the data for drift (on timescales ranging from 4 to 10 h) in the detector response [e.g., *Sive*, 1998; *Wang et al.*, 1999; *Colman et al.*, 2001; *Zhou*, 2006]. If the response factor used for converting detector response (area units) to mixing ratios was changing with time, this was confirmed by comparing the amount of drift in the other calibrated standards analyzed during the project. A best-fit line (linear for CH_2Br_2 and $CHBr_3$ on both analytical systems) was fit to a plot of the detector response to the standards versus the time of injection. The fit was then normalized to its mean value to give the relative detector response line. Both standards were employed for each compound quantified, and their respective relative detector response factor lines were averaged for each system. The relative detector response line was then scaled to the average detector response per mixing ratio calculated from the calibrated standard runs. Finally, when quantifying samples, the appropriate absolute response factor for each detector was determined from the appropriately scaled detector response line and the time of sample injection. The detector response to a sample was then divided by this value to give an absolute mixing ratio. The resulting measurement precision for CH_2Br_2 and $CHBr_3$ in the sets of standards analyzed during the ICARTT campaign for each analytical system are listed in Table 2.

[17] Although evaluation of the whole air standards represents a reasonable way to estimate the precision of our analytical systems, it only tells us how precisely a component of a specific mixture (in this case two mixtures for each system) of compounds can be measured. Under ideal conditions, the approach to calculating experimental precision outlined above is robust and firmly rooted in probability statistics; however, our experience during the ICARTT campaign was not ideal because TF suffered a power outage on 21 July 2004. It took several days to repair the cause of the outage and reestablish proper operation of the GC instrument. Thus, another approach that can be used for estimating the analytical precision is to calculate the relative standard deviation of samples thought to have been collected in a homogeneous air mass [e.g., *Wingenter et al.*, 1996,

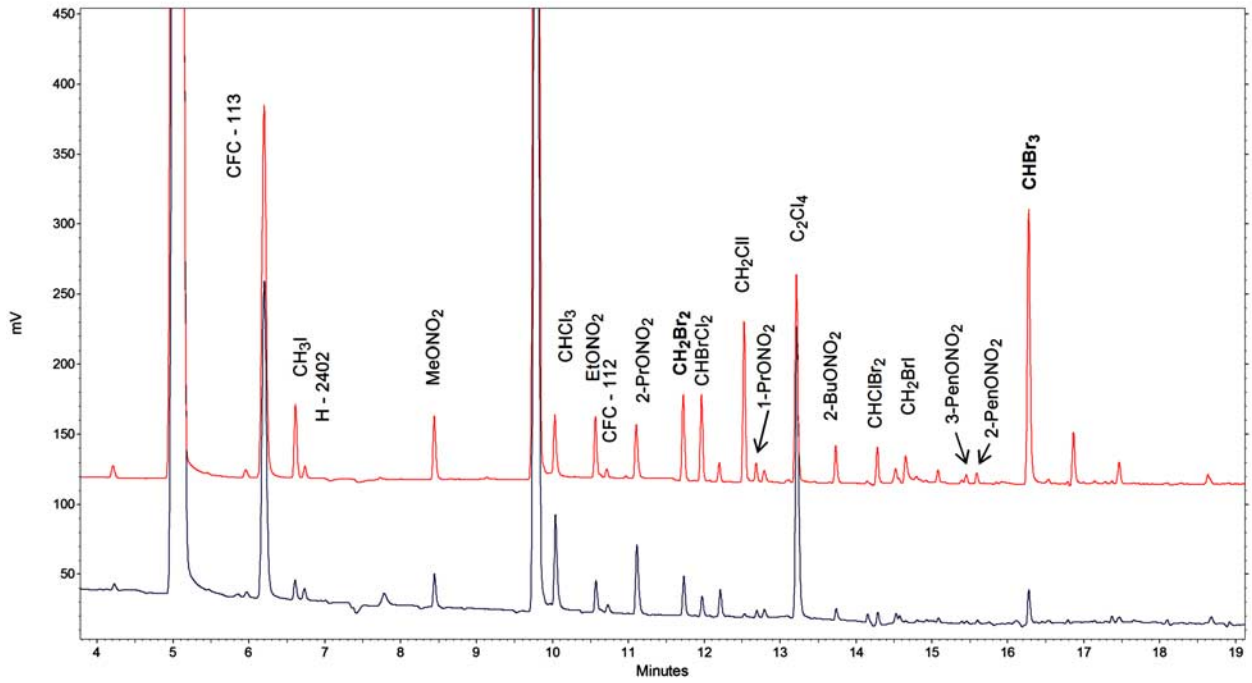

Figure 3. Chromatograms from samples collected on Appledore Island on 12 July 2004 at 0600 EDT (EDT in this paper is equivalent to local time) (blue) and 11 August 2004 at 0500 EDT (red). The CH_2Br_2 and $CHBr_3$ mixing ratios for the corresponding samples were 1.9, 7.7 and 5.5, 34.8 pptv, respectively.

1999, 2005; *Colman et al.*, 2001; *Schauffler et al.*, 1999, 2003; *Swanson et al.*, 2003]. For ease in comparing the measurement precision of CH_2Br_2 and $CHBr_3$ for both systems employed during the ICARTT campaign, the analytical precision is also estimated from the 4-d study conducted in June 2004. During this time period, a clean, relatively homogeneous air mass was encountered for approximately 24 h that spanned from 3 to 4 June (Figure 2a, shaded area). Different time intervals are used to evaluate the analytical precision of CH_2Br_2 and $CHBr_3$ corresponding to periods when each gas demonstrated a minimum in its temporal variability. For CH_2Br_2, a 12-h period was evaluated spanning from 3 June (1200 EDT) (EDT in this paper is equivalent to local time) to 4 June (0000 EDT). The resulting CH_2Br_2 homogeneous air mass measurement precision for the TF GC was 3.4% (1.30 ± 0.04 pptv) while the canister samples yielded a precision of 2.5% (1.26 ± 0.03 pptv). For $CHBr_3$, a 5-h period from 0800 to 1300 on 4 June was assessed for estimating the measurement precision. For the TF GC, the analytical precision was 4.0% (1.50 ± 0.06 pptv) while the canister system was 2.3% (1.54 ± 0.04 pptv). In comparing these two methods for evaluating each system's performance, we consider the whole air standard-derived precision to reflect the overall measurement precision achieved within the range of the working standards over the course of the entire six week campaign while the homogeneous air mass precision to be an estimate of the measurement precision achieved during a shorter time interval (ranging from 4–6 h).

2.2.5. CH_2Br_2 and $CHBr_3$ Calibrations

[18] To illustrate the wide range of air mass variability observed during the ICARTT campaign, chromatograms from the OV-1701 ECD channel for two samples collected at Appledore Island are shown in Figure 3. The large variation in peak size between the two samples reflects the difference between continental outflow, with low levels of CH_2Br_2 and $CHBr_3$, and that of pronounced marine influence during Tropical Storm Bonnie. The contrast between air mass regimes qualitatively illustrates the dynamic range for the bromocarbon measurements.

[19] The absolute accuracy for the whole air standards used during ICARTT was ±10% for both CH_2Br_2 and $CHBr_3$ on the basis of primary reference halocarbon standards generated from static dilutions of pure compounds prepared in the UCI laboratory [*Wang*, 1993]. Calibrations for the TF GC and the canister samples were carried out by determining response factors from a series of calibrated whole air and synthetic standards. The whole air working standards employed have mixing ratios representative of urban and clean free tropospheric air, thus bracketing the high and low ranges for the expected observations. Furthermore, linearity studies were conducted to evaluate detector response over the observed mixing ratio ranges for all classes of compounds. Results from the linearity studies for CH_2Br_2 and $CHBr_3$ are shown in Figure 4 for both the TF GC and canister system. For both analytical systems, the ECD response was linear over the observed mixing ratio ranges during the ICARTT campaign.

[20] Each of the whole air working standards used for the TF GC and canister system were purchased from UCI and were calibrated by D. Blake. The mixing ratios for halocarbons, NMHCs and alkyl nitrates have been verified by B. Sive on an independent analytical system at the University of New Hampshire. Our calibration scheme has been cross-checked against absolute standards from other research groups for hydrocarbons, halocarbons and alkyl nitrates.

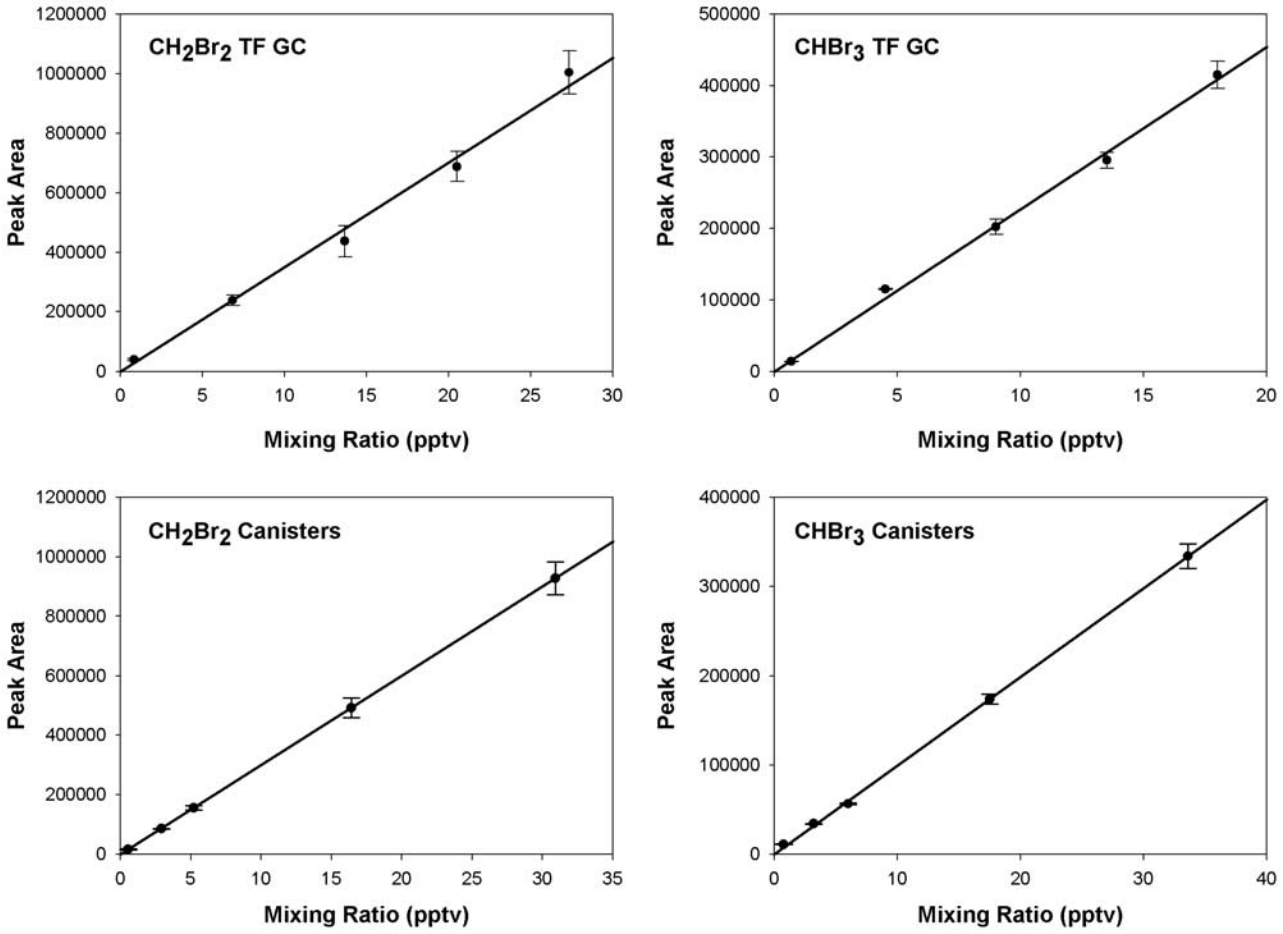

Figure 4. A series of calibration curves for CH_2Br_2 and $CHBr_3$ using calibrated whole air standards during the ICARTT campaign. The calibration curves were generated from the OV-1701 ECD channel for both the TF GC and the canister system. Each data point represents the average of three measurements. The vertical bars represent the standard deviation of the three measurements.

Furthermore, the group at UCI has participated in numerous intercomparison experiments, and their analytical procedures consistently yielded accurate identification for a wide range of unknown VOCs and have produced excellent quantitative results. Moreover, the working standards are part of the larger network of whole air standards maintained by B. Sive at UNH as part of the AIRMAP program. In total, there are currently 10 high-pressure cylinders, six 36-liter electropolished low-pressure pontoons (~350 psi), and three 32-liter electropolished high-pressure pontoons (~900 psi) containing whole air standards that have been filled and calibrated by UCI and independently verified by UNH.

[21] The six 36-liter electropolished low-pressure pontoons containing calibrated whole air standards are analyzed regularly with the high-pressure cylinders to reverify their mixing ratios because they are susceptible to changes in composition over long periods of time. Regular analysis of the cylinders and low-pressure pontoons enables us to monitor any mixing ratio drift in the cylinders that may occur with time. The low-pressure pontoons are proven reliable and show minimal changes in composition over a period of years for most gases. Additionally, the mixing ratios of the cylinders and low-pressure pontoons are cross-referenced to the three 32-liter electropolished high-pressure pontoons containing calibrated whole air standards. The high-pressure pontoons, in conjunction with the low-pressure pontoons, are the basis of the long-term calibration scale for AIRMAP and are used to ensure consistent calibration scales for the VOC measurements conducted at multiple sampling sites. Additionally, the high-pressure pontoons are periodically compared with additional standards from D. Blake at UCI for halocarbon, NMHC and alkyl nitrate mixing ratio verification. Intercomparing standards, both formally and informally, has helped to ensure that measurements from different research groups on various platforms were on the same or similar calibration scale during ICARTT, making it possible to meaningfully compare the AIRMAP measurements with those generated by other research groups.

3. Atmospheric Distributions of Marine-Derived Halocarbons

[22] Figure 5 shows the time series of $CHBr_3$ and CH_2Br_2 measured during three consecutive summers at TF (2002–2004) and at AI (2004). The mean, maximum, and minimum mixing ratios of $CHBr_3$ and CH_2Br_2 at these two sites are

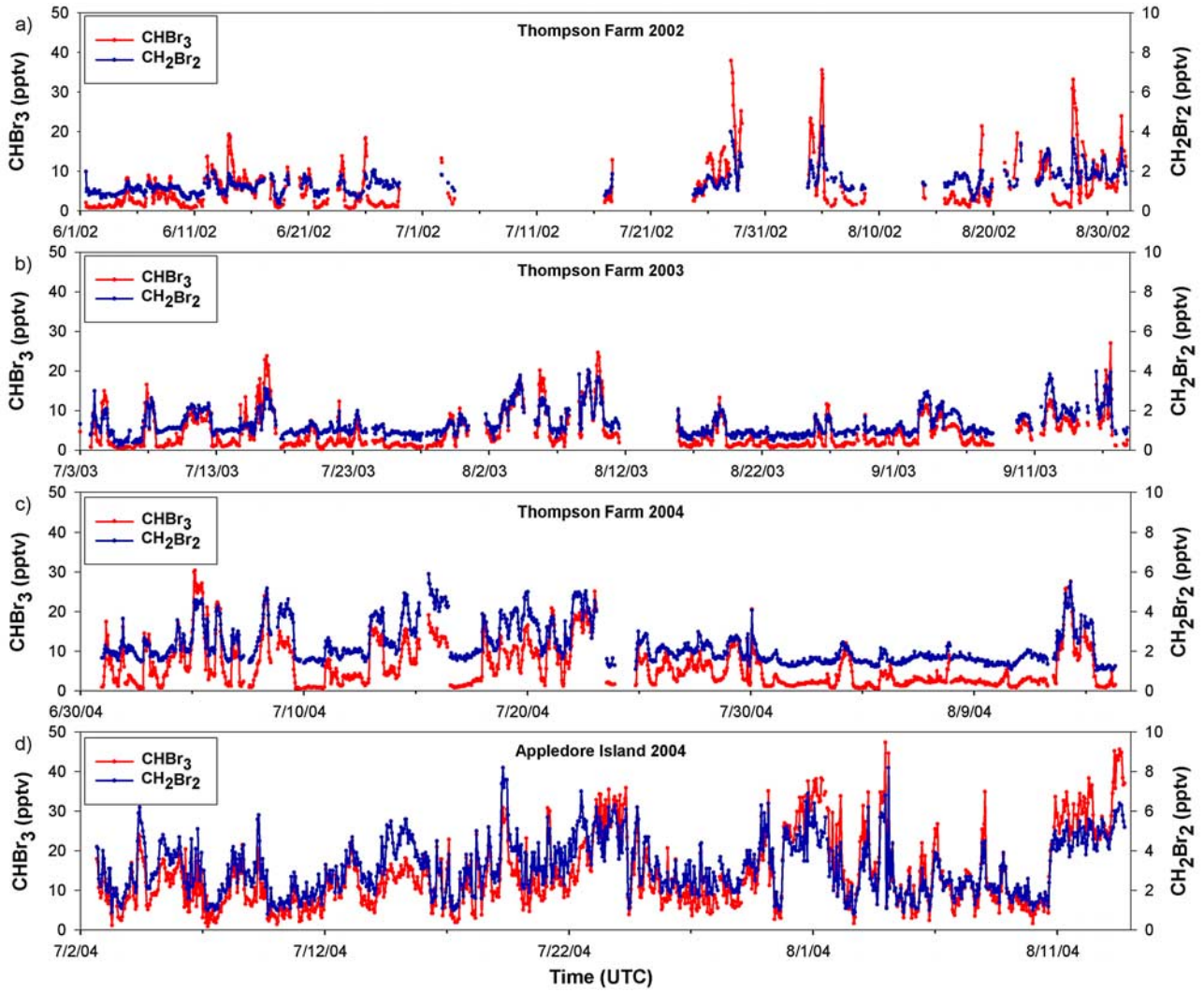

Figure 5. Time series of $CHBr_3$ and CH_2Br_2 at (a) Thompson Farm during the summer of 2002, (b) Thompson Farm during the summer of 2003, (c) Thompson Farm during the summer of 2004, and (d) Appledore Island during the summer of 2004.

listed in Table 3. During the study periods, $CHBr_3$ and CH_2Br_2 were well correlated at both sites, indicating their similar sources (Figure 5). Much greater variability of $CHBr_3$ compared with CH_2Br_2 is shown by its higher relative standard deviations (Table 3) and likely results from variable production rates in the surface seawater and its higher reactivity in the atmosphere. Additionally, lower background tropospheric mixing ratios of $CHBr_3$ corroborates that large mixing ratio enhancements resulting from the higher production rates in the coastal environment are further driving its greater variability as compared to CH_2Br_2.

[23] Elevated concentrations of $CHBr_3$ and CH_2Br_2, as determined by the 75th percentile, were frequently observed at these two sites, with values ranging from 7.7–9.5 pptv ($CHBr_3$) and 1.6–2.7 pptv (CH_2Br_2) for TF (summers of 2002–2004) and 18.2 pptv ($CHBr_3$) and 4.2 pptv (CH_2Br_2) at AI (summer of 2004) (Table 3). Previous studies in this region found that air masses encountered at TF are frequently influenced by emissions from coastal and estuarine waters [*Zhou et al.*, 2005]. At TF, mean mixing ratios during these periods ranged from 5.3–6.3 pptv for $CHBr_3$ and 1.3–2.3 pptv for CH_2Br_2 (Table 3). These values are comparable

Table 3. Statistics for $CHBr_3$ and CH_2Br_2 at Thompson Farm and Appledore Island[a]

		$CHBr_3$, pptv						CH_2Br_2, pptv						
		Max	Min	25% Percentile	75% Percentile	Mean	RSD, %	Max	Min	25% Percentile	75% Percentile	Mean	RSD, %	N
Thompson Farm	1 June to 31 August 2002	38	0.6	1.8	8.0	5.9	99	4.2	0.4	1.0	1.6	1.4	40	810
	3 July to 15 August 2003	24.6	0.2	1.4	7.7	5.3	98	4.0	0.2	0.9	1.7	1.3	51	658
	2 July to 15 August 2004	30	1.0	2	9.5	6.3	91	5.9	0.5	1.6	2.7	2.3	43	1304
Appledore Island	2 July to 13 August 2004	47	0.9	7.7	18.2	14.3	64	8.2	0.8	2.1	4.2	3.2	44	1001

[a]RSD is the relative standard deviation.

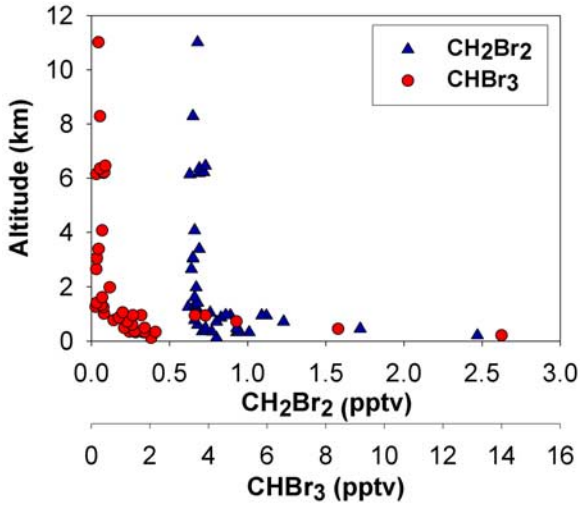

Figure 6. Vertical distributions of $CHBr_3$ and CH_2Br_2 during the ICARTT 2004 campaign. The data points shown encompass the coastal region of the Gulf of Maine, TF and AI.

with previously reported results from coastal regions between 40°–60°N [*Carpenter et al.*, 2003; *Quack and Wallace*, 2003; *Yokouchi et al.*, 2005; *Zhou et al.*, 2005]. The mean mixing ratios of both gases were higher at AI ($CHBr_3$ = 14.3 pptv, CH_2Br_2 = 3.2 pptv) compared to TF ($CHBr_3$ = 6.3 pptv, CH_2Br_2 = 2.3 pptv) during the ICARTT campaign indicating the influence of local marine sources on the composition of air masses in this region (Figures 5c and 5d, Table 3).

[24] Figure 6 shows the tropospheric vertical distributions of $CHBr_3$ and CH_2Br_2 measured onboard the NASA DC-8 aircraft as part of INTEX-NA during the ICARTT campaign. The data points shown correspond to samples taken when the aircraft was within 42.0–43.5°N and 69.5–71.0°W, which encompasses the coastal region of the Gulf of Maine and includes TF and AI. The mixing ratios measured at altitudes below 1 km spanned from 0.8 to 14.0 pptv (mean = 2.9 pptv) and 0.7 to 2.5 pptv (mean = 1.0 pptv) for $CHBr_3$ and CH_2Br_2, respectively. At altitudes above 1 km, mixing ratios ranged from 0.2 to 1.1 pptv (mean = 0.4 pptv) and 0.6 to 0.8 pptv (mean = 0.7 pptv) for $CHBr_3$ and CH_2Br_2, respectively. Both gases consistently exhibited strong, negative vertical gradients from the boundary layer to the lower free troposphere (Figure 6) with a faster decrease observed in $CHBr_3$. The difference in $CHBr_3$ mixing ratios between the marine boundary layer (MBL) and free troposphere (FT) (600%) was significantly larger than that for CH_2Br_2 (30%). To the best of our knowledge, the sources for these two compounds exist near the surface, and because $CHBr_3$ has a relatively short lifetime resulting from photochemical loss, it is likely that the reduction in mixing ratio with altitude results from vertical mixing and/or chemical loss.

4. Correlations of Marine Halocarbons

[25] Mixing ratios of $CHBr_3$ and CH_2Br_2 were well correlated at TF and AI, illustrating the persistence of their common marine sources throughout the region (Figure 7). The slopes for all four data sets were determined by orthogonal distance regression (ODR) which accounts for uncertainties in both the x and y variables. The average slope of CH_2Br_2 versus $CHBr_3$ from the ODR analysis was 0.14 ± 0.01 for all four data sets and is within the range of reported emission ratios for coastal regions. It is worth noting that when $CHBr_3$ and CH_2Br_2 mixing ratios at AI were above ~20 pptv and ~5 pptv, respectively, the ratio of these two gases deviated from the linear fit through the entire data set, which indicates the effect of direct emissions from the surface seawater (Figure 7). The difference in the slopes of these two regimes may provide additional insight regarding air mass processing and transport, warranting further investigation. However, a linear fit is used here to compare the $CH_2Br_2/CHBr_3$ ratio derived from our measurements to other values reported in the literature. *Carpenter et al.* [2003] obtained an average emission ratio of 0.15 at Mace Head, Ireland, which is strongly influenced by local macroalgae, while *Yokouchi et al.* [2005] estimated the $CH_2Br_2/CHBr_3$ emission ratio to be approximately 0.11. Comparison between $CH_2Br_2/CHBr_3$ ratios in our study and those reported in previous studies suggests that the $CHBr_3$ and CH_2Br_2 measurements at TF and AI are influenced by biogenic sources (e.g., macroalgae beds) in the local coastal waters [*Zhou et al.*, 2005]. The nonzero intercepts in Figure 7 reflect the longer lifetime and slower removal of CH_2Br_2 relative to $CHBr_3$, resulting in a nonzero CH_2Br_2 background mixing ratio when extrapolated to zero $CHBr_3$. As a result, average tropospheric mixing ratios of CH_2Br_2 (0.8–3.4 pptv) are estimated to be similar or higher than those of $CHBr_3$ (0.6–3.0 pptv) [*World Meteorological Organization*, 2003].

[26] The emission of $CHBr_3$ has been estimated to be 6–7 times larger than that of CH_2Br_2, resulting in higher $CHBr_3$ mixing ratios near source regions (e.g., Figure 6). Our measurements are in good agreement with this estimate as illustrated by the values of the slopes determined by ODR in Figure 7. Because the $CH_2Br_2/CHBr_3$ ratio in background air masses is higher than those in close prox-

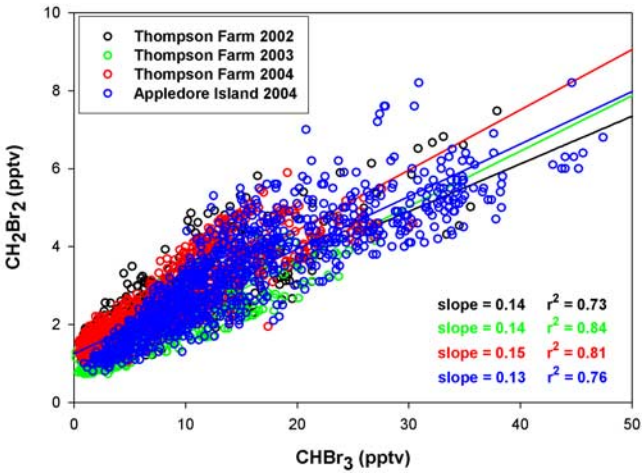

Figure 7. Correlations between $CHBr_3$ and CH_2Br_2 at Thompson Farm (2002–2004) and Appledore Island (2004).

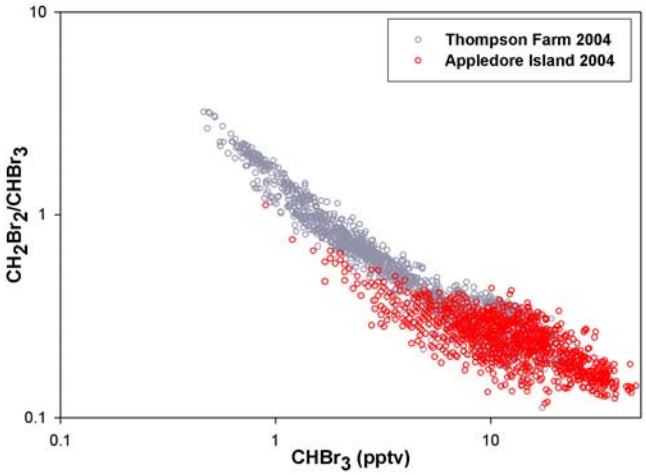

Figure 8. Relationships between $CH_2Br_2/CHBr_3$ ratios and $CHBr_3$ mixing ratios at Thompson Farm (gray) and Thompson Farm and Appledore Island (red).

imity to source regions, when the air mass is transported away from the source region, dilution will independently increase the slope of the ratio until it approaches the value for background air. Faster photochemical removal of $CHBr_3$ relative to CH_2Br_2 can also increase the slopes of the regression lines. At locations in close proximity to sources, the change in the slope is caused by dilution with background air, allowing little or no reactive loss during transport, while at locations far from source regions, the slope is affected by chemical decay during a long period of transport [*Yokouchi et al.*, 2005].

[27] Although the measured mixing ratios were higher at AI compared to TF, the difference in the slopes from the regression of CH_2Br_2 versus $CHBr_3$ were not statistically significant (0.13 at AI versus 0.15 at TF), illustrating the pervasiveness of the marine influence throughout the region (Figure 7). However, air masses sampled at AI had more recent marine influences because of the close proximity to sources. This is clearly seen by analyzing the relationship between $CH_2Br_2/CHBr_3$ and $CHBr_3$, as illustrated in Figure 8. A wide range of $CH_2Br_2/CHBr_3$ ratios were observed, indicative of the variety of air masses and atmospheric processes encountered at both sites (Figure 8). In general, air masses had lower $CH_2Br_2/CHBr_3$ ratios at AI compared to TF reflecting the close proximity to fresh emissions from the coastal waters. The $CH_2Br_2/CHBr_3$ ratio decreased with increasing $CHBr_3$ mixing ratios reflecting that air masses with recent marine influences tend to have a higher fraction of $CHBr_3$ than those with less recent marine influences, which is likely a result of the differences in their chemical reactivities. The photochemical removal of $CHBr_3$ is faster than that of CH_2Br_2, thus, the fraction of $CHBr_3$ in an air mass tends to decrease with time when transported away from the source region. However, photochemical removal alone cannot explain the observed differences in the $CH_2Br_2/CHBr_3$ ratios at TF and AI. In order to evaluate the subtle differences in ratios observed between both locations, we have calculated the expected $CH_2Br_2/CHBr_3$ ratio in air masses that are transported inland from AI to TF. To simulate the air mass transport, we have only included the measurements corresponding to time periods when the winds were from the southeast at both sampling sites. The calculation for the expected $CH_2Br_2/CHBr_3$ ratio is based on the photochemical lifetimes of CH_2Br_2 (2 months) and $CHBr_3$ (2 weeks) and the observed average $CH_2Br_2/CHBr_3$ ratio at AI from the southeast wind sector (0.12). The calculated results illustrate that if only photochemical removal is included, it would take ~80 h for the ratio to change from 0.12 to 0.15, which is the average ratio observed at TF. However, the timescale for transporting air masses from AI to TF is on the order of ~1.5 h under typical conditions with wind speed of 6 m s^{-1} [*Mao et al.*, 2006], corresponding to a small percentage increase in the $CH_2Br_2/CHBr_3$ ratio. This implies that the differences observed in the $CH_2Br_2/CHBr_3$ ratio versus $CHBr_3$ between TF and AI are likely due to the mixing of air masses with background air having lower mixing ratios of $CHBr_3$ and subsequently a higher $CH_2Br_2/CHBr_3$ ratio.

5. Source Region Relationships

[28] The mean mixing ratios of $CHBr_3$, CH_2Br_2, tetrachloroethene (C_2Cl_4) and trichloroethene (C_2HCl_3) in air masses arriving from the four primary wind sectors at TF, and five wind sectors at AI are illustrated in Figure 9. Because of its geographical location (Figure 1), the southwest wind sector (180–270°) at AI has been subdivided into two different categories: 180–225° and 225–270°, which represent coastal and continental influences, respectively.

[29] At TF (2002–2004), air masses arriving from the northeast (NE) (0–90°) and southeast (SE) (90–180°) wind sectors had average $CHBr_3$ mixing ratios ranging from 8.2–12.6 pptv, while mixing ratios in air masses from the southwest (SW) (180–270°) and northwest (NW) (270–360°) varied from 3.8–4.8 pptv (Figures 9a–9c). For CH_2Br_2, mean mixing ratios in the NE and SE sectors were higher (1.4–3.0 pptv) than those from the SW and NW sectors (0.9 to 2.0 pptv) at the 95% confidence level (Figures 9a–9c). In all cases, air masses transported from the NE and SE had higher average levels of $CHBr_3$ and CH_2Br_2 (approximately 70–220% and 20–90%, respectively) than those from the SW and NW sectors, because air flow patterns from the NE and SE sectors pass over the estuarine and coastal marine regions. The difference in the mean CH_2Br_2 mixing ratios between the different wind sectors compared to that in $CHBr_3$ reflects that its emissions are smaller than $CHBr_3$ emissions, leading to the smaller variations observed. Additionally, because the lifetime of CH_2Br_2 is much longer than that of $CHBr_3$, it is relatively well mixed throughout the troposphere.

[30] Both C_2Cl_4 and C_2HCl_3 are widely used as dry cleaning fluids and solvents [*Wang et al.*, 1995], and are frequently used as tracers of urban air masses [*Blake et al.*, 1996b]. The atmospheric lifetimes of C_2Cl_4 and C_2HCl_3 are ~3.5–4 months and ~7 d, respectively [*Singh et al.*, 1996; *Quack and Suess*, 1999; *Olaguer*, 2002]. The lowest average concentrations of C_2Cl_4 and C_2HCl_3 were associated with flow from the NE and NW sectors at both sites, suggesting transport of cleaner Canadian air masses to the study region [*Moody et al.*, 1998; *Mao and Talbot*, 2004]. The low levels of C_2Cl_4 and C_2HCl_3 and corresponding

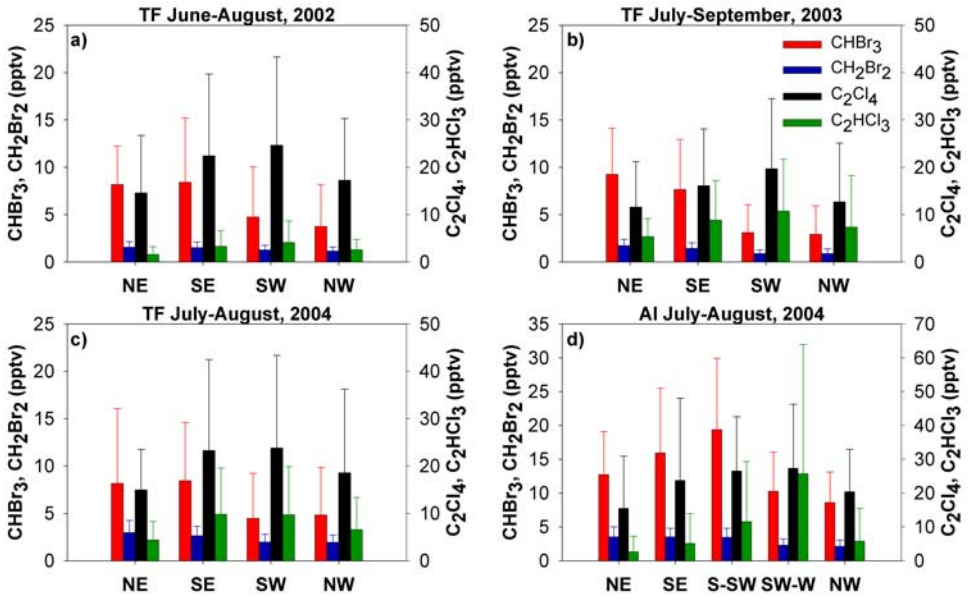

Figure 9. Average mixing ratios of $CHBr_3$, CH_2Br_2, C_2Cl_4, and C_2HCl_3 partitioned by wind sector from (a) Thompson Farm, 2002, (b) Thompson Farm, 2003, (c) Thompson Farm, 2004, and (d) Appledore Island, 2004. The vertical bars represent the standard deviation.

high levels of $CHBr_3$ and CH_2Br_2 from the NE sector at both sites are consistent with their different source strengths. Mixing ratios of C_2Cl_4 and C_2HCl_3 were higher in the SW and SE sectors at TF and the SW-W (225–270°) sector at AI compared to those in other wind sectors. These results clearly reflect the pronounced anthropogenic influences on air masses traveling north from the northeastern urban corridor, in agreement with the findings from *Mao and Talbot* [2004]. Additionally, the elevated C_2Cl_4 and C_2HCl_3 levels correlate well with the higher average ozone (O_3) mixing ratios from the corresponding wind sectors for TF and AI (see section 7.2). Although air masses originating from the SE at TF (SE and S-SW at AI) possessed the chemical characteristics of coastal marine influence, they also exhibited higher average concentrations of C_2Cl_4 and C_2HCl_3 compared to air masses from the NW and NE sectors. It is likely that this unique chemical signature results from the export of polluted air masses originating in the mid-Atlantic states, as suggested by *Mao and Talbot* [2004]. More specifically, while air masses were transported out of the mid-Atlantic states moving northeastward over the ocean, the flow was constantly mixed with the fresh emissions in the continental outflow from major metropolitan areas, such as Boston and New York. Under the influence of the subtropical high and Canadian low-pressure system, the flow would make landfall in northeastern New England, most likely bearing high levels of anthropogenic tracers [*Mao and Talbot*, 2004]. The typical back trajectories shown in Figure 14, which are discussed further in section 7.2, illustrate the complexity of the dynamical processes occurring in this region.

[31] The overall trends observed at AI were similar to those of TF with the highest average $CHBr_3$ and CH_2Br_2 mixing ratios occurring when flow was from the NE, SE, and S-SW (180–225°) wind sectors, which are influenced by the marine environment (Figure 9d). Furthermore, the SE and S-SW wind sectors represent open-ocean and coastal water influences, respectively, and on average, mixing ratios of $CHBr_3$ were 20% higher for the S-SW sector compared to the SE sector. These findings indicate that the coastal marine sources are more significant compared to those of the open ocean. Moreover, these results are in good agreement with our measurements of surface seawater concentrations and estimates of sea-to-air fluxes in the Gulf of Maine during the New England Air Quality Study (NEAQS) 2002 campaign, where the highest surface seawater concentrations and fluxes of $CHBr_3$ were along the coastal region of New Hampshire [*Zhou et al.*, 2005].

6. Sea-to-Air Transfer

[32] Figure 10 shows the relationship of wind speed versus $CHBr_3$ and CH_2Br_2 mixing ratios at AI. The data set has been partitioned by wind speed into 12 intervals at increments of 1 m s^{-1} from 0–11 m s^{-1}. The wind speeds and mixing ratios for both gases were averaged over each interval. For wind speeds >11 m s^{-1} (maximum = 12.8 m s^{-1}), the mixing ratios and wind speeds were averaged over the 11–12.8 m s^{-1} interval. As shown in Figure 10, $CHBr_3$ and CH_2Br_2 mixing ratios increased with wind speed in the coastal marine environment, facilitating the sea-to-air flux of these dissolved gases. The relationship between wind speed and sea-to-air fluxes for dissolved trace gases can be described by

$$F = k_w(C_w - C_a/H), \quad (1)$$

where F is the flux across the air-sea interface, k_w is the gas transfer coefficient, C_w and C_a are the concentrations in the surface seawater and air, respectively, and H is the dimensionless Henry's law constant. The transfer coefficient

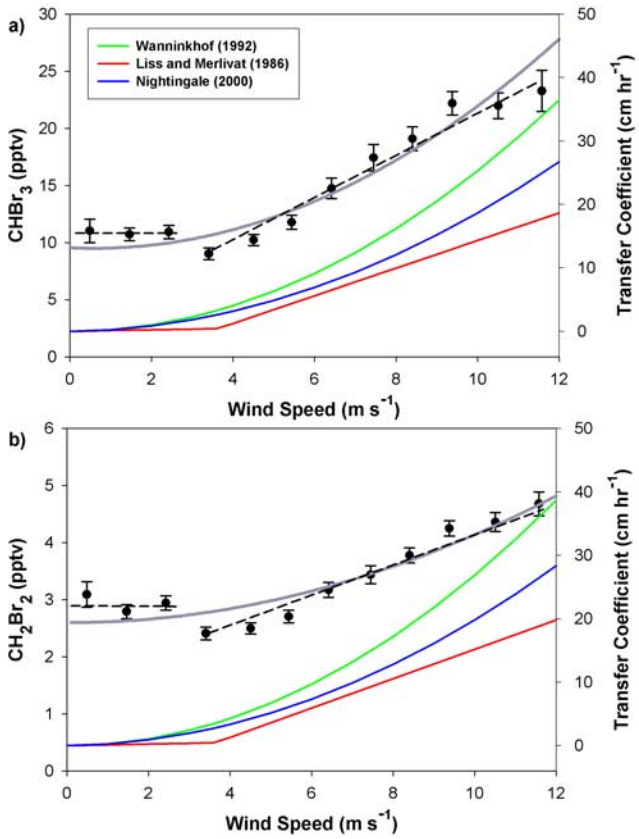

Figure 10. Relationship between wind speed and mixing ratios of (a) $CHBr_3$ and (b) CH_2Br_2, at Appledore Island during the summer 2004. The error bars shown are the standard deviation of the mean for the average mixing ratios. Linear and second-order polynomial fits were applied to the data to illustrate the difference between the smooth surface and rough surface regimes. Also shown are the sea-to-air exchange transfer coefficients (cm h^{-1}) versus wind speed for $CHBr_3$ (Figure 10a) and CH_2Br_2 (Figure 10b) using parameterizations from *Wanninkhof* [1992], *Liss and Merlivat* [1986], and *Nightingale et al.* [2000].

k_w depends on the wind speed, the identity of the gas, water temperature and salinity.

[33] The sea-to-air transfer coefficients for $CHBr_3$ and CH_2Br_2 using three different parameterizations from the literature are shown in Figure 10. Each of these parameterizations show consistent features in the transfer coefficient for each gas as a function of wind speed. The parameterizations from *Wanninkhof* [1992] and *Nightingale et al.* [2000] are polynomial models that assume the flux of a compound, which is supersaturated with respect to the liquid phase, increases with water temperature and wind speed. *Wanninkhof* [1992] described a parameterization of the transfer coefficient suitable for $CHBr_3$ as

$$k_{w\,\mathrm{CHBr3}} = 0.31\ u^2 (660/Sc_{\mathrm{CHBr3}})^{1/2}, \tag{2}$$

where u is the instantaneous wind speed in m s^{-1} and Sc is the Schmidt number, which incorporates the kinematic viscosity of the solvent and diffusion coefficient of the compound of interest. The parameterization of the transfer coefficient for CH_2Br_2 can also be established in a similar manner. This parameterization of the transfer coefficient was used in our previous work [*Zhou et al.*, 2005] for comparison with other previously reported results [*Quack and Wallace*, 2003]. Similarly, the sea-to-air transfer coefficient k_w can be calculated using the equation of *Nightingale et al.* [2000] as

$$k_w = \left(0.23\ u^2 + 0.1\ u\right)(Sc/600)^{-1/2}. \tag{3}$$

[34] The parameterization of *Liss and Merlivat* [1986] is a conditional model, which produces different values of k_w for different oceanic regimes: (1) low wind speeds with minimal waves (smooth surface regime), (2) moderate wind speeds and wave activity (rough surface regime), and (3) high wind speeds and whitecap waves (breaking wave regime). Up to wind speeds of ~3–5 m s^{-1} the value of k_w increases very gradually. For the rough surface regime (~5–13 m s^{-1}), the presence of waves considerably increases the slope of the k_w versus wind speed. Above wind speeds of ~13 m s^{-1}, bubbles become prevalent resulting from breaking waves, further increasing sea-to-air gas transfer. *Liss and Merlivat* [1986] proposed the following three relationships for the variation of k_w with wind speed in the marine environment:

$$k_w = 0.17\ u, \qquad \mathrm{u} \le 3.6\ \mathrm{m\,s^{-1}}, \tag{4}$$

$$k_w = 2.85\ u - 9.65, \qquad 3.6\ \mathrm{m\,s^{-1}} < \mathrm{u} \le 13\ \mathrm{m\,s^{-1}}, \tag{5}$$

$$k_w = 5.9\ u - 49.3, \qquad \mathrm{u} > 13\ \mathrm{m\,s^{-1}}, \tag{6}$$

where u is the instantaneous wind speed in m s^{-1}. The *Liss and Merlivat* [1986] model is based on carbon dioxide (CO_2) exchange; other gases can be estimated from the Schmidt number ratio of the gas under consideration to CO_2. Thus, the transfer velocity k'_w for other gases may be approximated with the *Liss and Merlivat* [1986] model by calculating $k'_w = k_w\,(Sc/600)^{-2/3}$, for $u < 3.6$ m s^{-1} or $k'_w = k_w\,(Sc/600)^{-1/2}$ for $u > 3.6$ m s^{-1}, which incorporates the kinematic viscosity of the solvent and diffusion coefficient of the compound of interest.

[35] According to equation (1), sea-to-air fluxes are expected to increase with wind speed. From our measurements at AI, a distinct wind speed relationship is observed for the entire data set (Figure 10). Mixing ratios in $CHBr_3$ and CH_2Br_2 varied little at wind speeds <3 m s^{-1}, increased proportionally at wind speeds ranging from 3–9 m s^{-1} and leveled off at wind speeds >9 m s^{-1}. In order to help understand the observed relationship between atmospheric mixing ratios and sea-to-air fluxes, the parameterizations of k_w from the models of *Wanninkhof* [1992], *Liss and Merlivat* [1986], and *Nightingale et al.* [2000] are also shown in Figure 10. Compared with the transfer coefficients from the *Liss and Merlivat* [1986] model, the pronounced demarcation shown in our measurements at ~3 m s^{-1} is similar to the model threshold of 3.6 m s^{-1}. These findings clearly illustrate the transition between the smooth surface and rough surface regimes. Moreover, the observed linear increase in mixing ratios at wind speeds ranging from 3–9 m s^{-1} is consistent with the modeled linear dependence of k_w for the

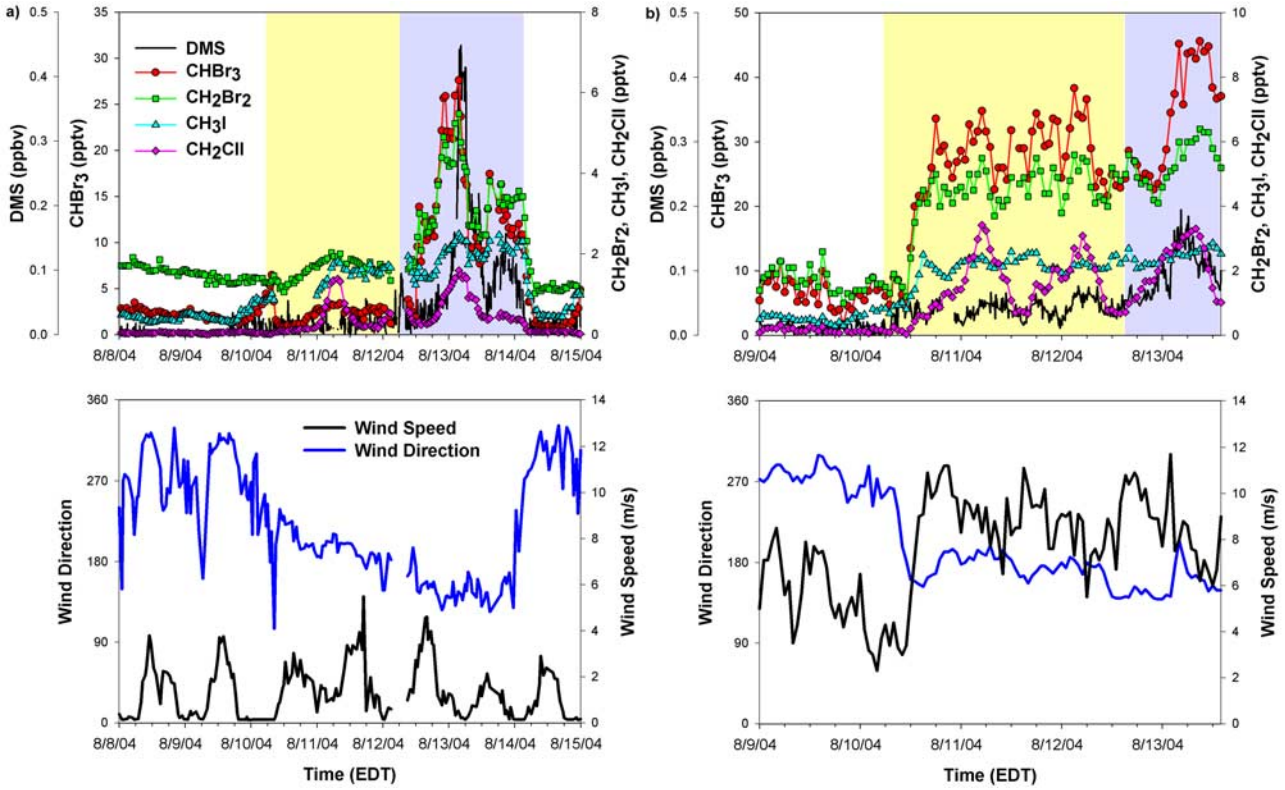

Figure 11. Mixing ratios of $CHBr_3$, CH_2Br_2, DMS, CH_3I, CH_2ClI, wind speed, and wind direction at (a) Thompson Farm and (b) Appledore Island, during Tropical Storm Bonnie. The tan shaded areas correspond to the pre–tropical storm period, and the blue shaded areas represent the time period when Tropical Storm Bonnie passed through the region.

rough surface regime. However, at high wind speeds (>9 m s^{-1}), the measurements begin to deviate from the modeled transfer coefficient, suggesting avenues for further investigation. Nonetheless, the robust correlation of mixing ratio with wind speed substantiates that $CHBr_3$ and CH_2Br_2 are emitted from the surface seawater in the Gulf of Maine.

[36] During the campaign the Gulf of Maine was impacted by remnants of Tropical Storm Bonnie passing through the northeastern United States. Wind speeds increased to ~10 m s^{-1} along the coastal region, which undoubtedly enhanced the sea-to-air transfer and the corresponding atmospheric mixing ratios of $CHBr_3$ and CH_2Br_2 at both AI and TF (see section 7.1). This impact was substantiated by the slight increase in average mixing ratios at TF compared to previous years (Table 3).

[37] Most of the wind speeds <3 m s^{-1} were observed between 2200 and 0900 EDT (~60%) with approximately 65% of these occurring between the hours of 2200 to 0500 (predawn darkness hours). Assuming that the MBL was relatively stable and the average temperatures were effectively constant during this period [*Mao et al.*, 2006], the concurrent halocarbon enhancements could be attributed to accumulation of those compounds in a less ventilated shallow MBL. Moreover, the lack of a photochemical removal mechanism at night could also contribute to the higher mixing ratios. From these results, it is clear that future studies including water concentrations (C_w in equation (1)) are needed to directly quantify the air-sea exchange of these marine-derived gases.

7. Case Studies

7.1. Influence of Tropical Storm Bonnie

[38] During the period from 10 to 14 August 2004, the northeastern United States was impacted by Tropical Storm Bonnie. Elevated mixing ratios of $CHBr_3$ and CH_2Br_2, in addition to other marine tracers, such as dimethyl sulfide (DMS), methyl iodide (CH_3I) and chloroiodomethane (CH_2ClI) [*Varner et al.*, 2008], were observed at both TF and AI beginning at midday on 10 August (Figure 11). As wind speeds from the southeast intensified, the sea-to-air transfer of marine-derived gases increased and the marine-influenced air masses were rapidly transported along the coast. The impact of this event was first observed at both sites on 10 August, when the wind direction shifted from the west to the southeast, indicating the counterclockwise circulation of the tropical storm traveling up the east coast. The tan shaded portions of Figures 11a and 11b correspond to the pre–tropical storm period, during which time somewhat elevated mixing ratios of the marine-derived gases were observed at both sites. The slight elevation in the marine-derived halocarbon mixing ratios observed during the pre–tropical storm period is likely associated with the rapid change in the wind direction from the west (continental outflow) to the southeast (marine flow). The blue shaded portions of Figures 11a and 11b show significantly higher mixing ratios associated with wind speed and wind direction, illustrating the impact of Tropical Storm Bonnie on the marine-derived gases. During the period spanning from 12

to 14 August, average mixing ratios of $CHBr_3$ and CH_2Br_2 were higher than those averaged over the summer of 2004 for the southeast wind sector (TF: $CHBr_3 \sim 50\%$, $CH_2Br_2 \sim 20\%$; AI: $CHBr_3 \sim 100\%$, $CH_2Br_2 \sim 40\%$).

[39] On 10 August at 1100 (EDT), the measured mixing ratios of $CHBr_3$ and CH_2Br_2 were 4.3 pptv and 1.2 pptv, respectively, at AI. By 1900, $CHBr_3$ and CH_2Br_2 mixing ratios increased to 28.5 pptv and 4.0 pptv, respectively. The higher mixing ratios of these gases resulted from increased wind speeds associated with Tropical Storm Bonnie, leading to larger sea-to-air fluxes (as discussed in section 6 and shown in Figure 10). From the best fit line of the linear regression for wind speeds above 3 m s^{-1} for $CHBr_3$ and CH_2Br_2 (Figure 10), a mixing ratio of 23.0 pptv was calculated for $CHBr_3$ at a wind speed of 10.8 m s^{-1} (1900), which was within 20% of our measured value of 28.5 pptv. For CH_2Br_2, the calculated mixing ratio at the same wind speed was 4.5 pptv compared to the measured value of 4.0 pptv. Although the measured mixing ratios for $CHBr_3$ and CH_2Br_2 during Tropical Storm Bonnie were comparable to the calculated mixing ratios using the best fit line for the entire AI data set, more observations are needed to further test the wind speed dependence relationship for these two gases during extreme weather events. Nonetheless, by using wind speed, concentration differences between the pre–tropical storm and tropical storm periods, and the marine boundary layer height, we have estimated the fluxes of these gases resulting from the increased wind speeds during Tropical Storm Bonnie's passage. The values are calculated using the linear relationship from Figure 10 (wind speed >3 m s^{-1}) between concentration (C) and wind speed (w) having a slope of s and intercept of b as follows:

$$C = b + s \times w. \tag{7}$$

Differentiating equation (7) with respect to time yields

$$\frac{dC}{dt} = s \times \frac{dw}{dt} = \text{Emission Flux/H}, \tag{8}$$

where H is the boundary layer height. Therefore, the emission flux is determined by

$$\text{Emission Flux} = \text{H} \times s \times \frac{dw}{dt}. \tag{9}$$

Because the boundary layer height at AI is not known for the tropical storm period, a value of 500 m has been chosen, which is a reasonable estimate for this location under normal conditions. For the tropical storm period, average fluxes of $CHBr_3$ and CH_2Br_2 were calculated to be 52.4 ± 21.0 nmol m^{-2} h^{-1} and 9.1 ± 3.1 nmol m^{-2} h^{-1}, respectively. The non–tropical storm period fluxes were approximately 18.9 ± 12.3 nmol m^{-2} h^{-1} for $CHBr_3$ and 2.6 ± 1.9 nmol m^{-2} h^{-1} for CH_2Br_2. The fluxes of $CHBr_3$ and CH_2Br_2 during the tropical storm were approximately 2–3 times larger than their background fluxes, and are on the same order of the increase in fluxes observed for CH_2ClI at AI [*Varner et al.*, 2008], which is expected because these three marine-derived gases follow the similar wind dependence as shown by equation (1). The non–tropical storm values are in good agreement with previous estimates for this region [*Zhou et al.*, 2005]. However, the flux estimates presented here largely depend on the boundary layer height, which is effectively not known because of the large-scale rapid vertical mixing during a tropical storm. Therefore, these fluxes should be viewed as lower limits and, for example, would be twice as large if the boundary layer height was increased to 1000 m, which may be a more appropriate value.

[40] The measurements from AI during this time period clearly illustrate that large fluxes of marine-derived gases were emitted into the atmosphere from the surface ocean during the passage of the tropical storm system. Figures 12a and 12b show the 3-d backward trajectories for 13 August 2004 at TF and AI. During its transit northward, Tropical Storm Bonnie traveled up the coastline, affecting the entire northeastern United States (Figures 12a and 12b). The extended period of high winds in contact with supersaturated coastal waters injected significant amounts of marine-derived compounds into the atmosphere. Because Tropical Storm Bonnie's path traveled primarily along the coastal waters of the east coast, it is likely that marine-derived halocarbons were emitted into the air mass in its transit northward, contributing further to the elevated atmospheric mixing ratios measured at AI. As illustrated in Figures 11 and 12, these compounds were rapidly transported from the costal zone to inland locations. Marine-derived halocarbons can play an important role in the chemistry of the atmosphere. Therefore, long-term event based observations of these gases under extreme weather conditions (i.e., tropical storms and hurricanes) may provide valuable information as the frequency and intensity of these events resulting from future climate change is currently not known.

7.2. Ozone Episodes and the Coastal Marine Influence at TF

[41] The multiyear data set from TF has provided a unique resource to evaluate the utility of using marine-derived halocarbons in characterizing O_3 episodes in the northeastern United States. From 3 July to 17 September 2003, 16 O_3 episodes with hourly maximum mixing ratios >60 ppbv were identified at TF, while 13 O_3 episodes (>60 ppbv) were encountered from 2 July to 14 August 2004. For the summers of 2003 and 2004, an O_3 mixing ratio of 60 ppbv corresponded to the 90th and 95th percentiles, respectively, and was chosen as the threshold value for elevated O_3 conditions to ensure sufficient data to carry out the analysis.

[42] Figure 13 shows $CHBr_3$ and O_3 mixing ratios along with wind direction and wind speed on 2 days when O_3 levels were >60 ppbv at TF. The temporal distributions for $CHBr_3$ and CH_2Br_2 were similar during these events; only the $CHBr_3$ results are presented here for clarity. In 2003, six of the sixteen O_3 episodes were characterized by enhanced $CHBr_3$ mixing ratios. During the ICARTT campaign, five of the thirteen O_3 events displayed similar enhancements in $CHBr_3$. For the summertime periods of 2003 and 2004, approximately 38% of all the O_3 episodes encountered at TF had enhanced $CHBr_3$ mixing ratios, in addition to other marine-derived gases. On 22 July 2004, elevated O_3 mixing ratios (maximum hourly O_3 average >110 ppbv) were observed during the afternoon (Figure 13a). The $CHBr_3$ mixing ratios measured during these time periods were considerably higher than the sampling period averages

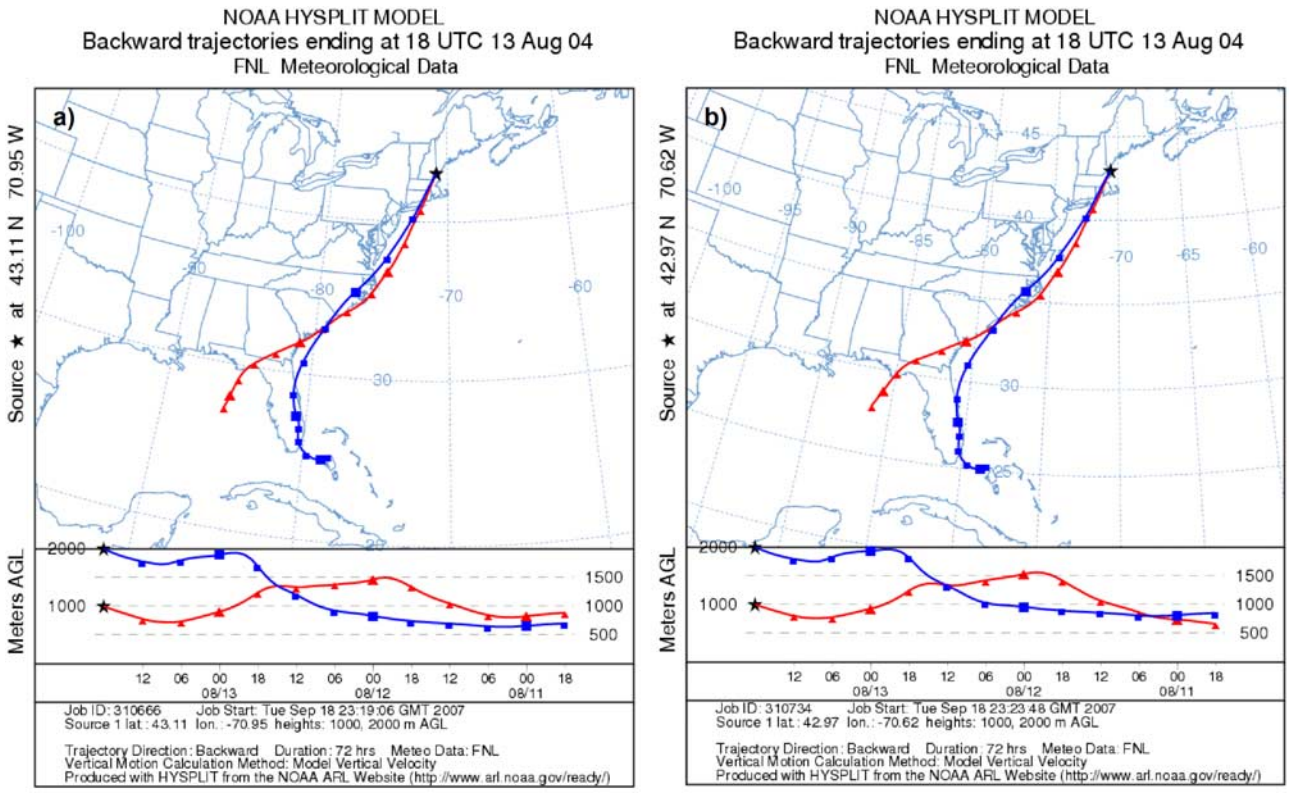

Figure 12. NOAA HYSPLIT backward trajectories for 13 August 2004 illustrating the coastal influence of the air mass arriving at (a) Thompson Farm and (b) Appledore Island (R. R. Draxler and G. D. Rolph, HYSPLIT (Hybrid Single-Particle Lagrangian Integrated Trajectory) model access via NOAA ARL READY Web site, http://www.arl.noaa.gov/ready/hysplit4.html, NOAA Air Resources Laboratory, Silver Spring, Maryland, 2005).

(Table 3), with hourly averages ranging from 12–25 pptv. Local meteorological data reveal that winds were from the SE, and air masses had passed over the coastal region, resulting in the elevated $CHBr_3$ mixing ratios observed during this high O_3 episode. The backward trajectory in Figure 14a illustrates that the air mass was influenced by both urban/industrial and coastal marine areas. The input of O_3 and its precursors into air masses transported from industrial areas likely contributed to the overall elevated O_3 levels measured at inland locations, such as TF. Coupled with the lack of O_3 deposition over the ocean and the potential for halogen atom chemistry in the coastal marine environment [e.g., *Keene et al.*, 2007; *Pszenny et al.*, 2007], the significance of these occurrences is that they frequently resulted in higher O_3 levels at TF compared with air masses originating from continental locations (e.g., air masses transported from the west).

[43] On 30 July 2004, O_3 mixing ratios were also elevated during the afternoon (maximum hourly O_3 average $\geq$90 ppbv). However, during this period, the mixing ratios of $CHBr_3$ were much lower than the sampling period average values listed in Table 3. For this particular O_3 episode, $CHBr_3$ mixing ratios ranged from 1.1–1.4 pptv and were close to background levels, such as when prevailing winds were from the SW and NW, indicating that air masses had little or no marine influence. The backward trajectory shown in Figure 14b suggests that the air mass was transported from the SW. Furthermore, the local meteorological data reveal that during this day, southwesterly winds prevailed, transporting O_3-rich air masses to TF (Figures 13b and 14b). The onshore flow with southeasterly winds was suppressed and its influence on inland pollutant loadings was minimized [*Mao and Talbot*, 2004].

[44] For the time periods spanning 3 July to 17 September 2003, and 2 July to 14 August 2004, approximately 60% of the O_3 episodes occurred under large-scale southwesterly flow patterns, solely having continental influences. On the basis of results from this study, more O_3 episodes were associated with continental influences than those with marine influences. However, because O_3 deposition over the ocean is not significant and there is the potential for halogen atom chemistry to further process air masses in the coastal marine environment [e.g., *Keene et al.*, 2007; *Pszenny et al.*, 2007], the magnitude of the O_3 levels during the marine influenced episodes was significant at inland locations and needs further investigation to determine the impact of coastal environments on chemical processing. Combining measurements of marine tracers with meteorological observations may ultimately prove useful in elucidating the proposed mechanisms about air mass transport in the coastal region and its effects on O_3 production.

[45] As discussed in section 5, *Mao and Talbot* [2004] demonstrated that the export of polluted air masses originating in the mid-Atlantic states, travels northeastward over the ocean, and is constantly mixed with the fresh emissions in the continental outflow from major metropolitan areas,

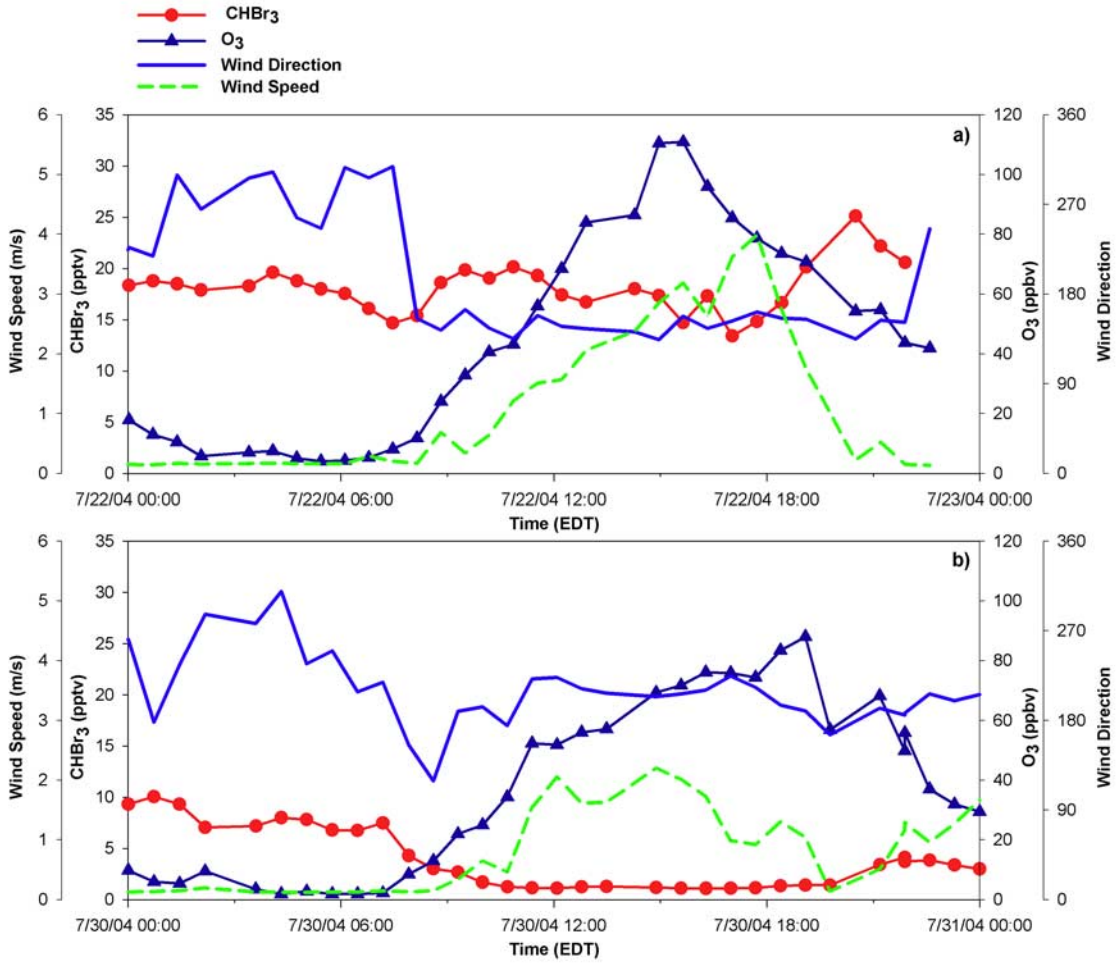

Figure 13. Mixing ratios of $CHBr_3$ and O_3, wind direction, and wind speed on selected days with hourly maximum O_3 > 60 ppbv at Thompson Farm on (a) 22 July 2004 and (b) 30 July 2004.

such as Boston and New York. Under the influence of the subtropical high and Canadian low-pressure system, the air masses make landfall in northeastern New England, most likely transporting high levels of pollutants. The results presented here provide clear evidence of the coastal marine influence and the "wrap around" transport pattern leading to high O_3 levels at inland locations in the northeast. Long-term observations and further analysis of these short-lived marine compounds could provide useful insight to our understanding of coastal zone influences on distributions of air pollutants. However, a further analysis of the frequency for which marine influences occur in air masses is needed to fully evaluate the importance of both marine and continental environments in shaping the coastal regional air quality and their contributions to O_3 formation.

8. Summary

[46] High concentrations of $CHBr_3$ and CH_2Br_2 were frequently observed at Thompson Farm and Appledore Island in the coastal and marine regions of northern New England, reflecting common sources associated with coastal water biogenic emissions. The AI marine site had higher concentrations of $CHBr_3$ and CH_2Br_2 compared to TF during the ICARTT 2004 campaign, illustrating the pronounced influence of local marine sources on their distributions. However, air masses encountered at TF also exhibited elevated levels of marine-derived gases from local coastal and estuarine water emissions. For 2002–2004, average mixing ratios of $CHBr_3$ and CH_2Br_2 at TF were generally comparable with previously reported results in coastal regions between 40°–60°N. Strong negative vertical gradients of $CHBr_3$ and CH_2Br_2 were observed in the troposphere over the coastal region of the Gulf of Maine, reflecting the surface oceanic sources of these gases. The rapid reduction in mixing ratios with altitude is a result of both photolytic loss and dilution by free troposphere air having low mixing ratios of $CHBr_3$ and CH_2Br_2.

[47] Common sources with similar emission ratios were corroborated by the robust correlations between $CHBr_3$ and CH_2Br_2 mixing ratios yielding similar slope values of the regression lines for all data sets from TF and AI. The $CH_2Br_2/CHBr_3$ ratios decreased with increasing $CHBr_3$ mixing ratios indicating that air masses with recent marine influences tended to have a higher fraction of $CHBr_3$ compared to those having less recent marine influences. Air masses generally had lower $CH_2Br_2/CHBr_3$ at AI than at TF, illustrating the pronounced local marine influences at AI.

[48] Large-scale circulation patterns play a critical role in controlling the distributions of trace gases in the atmo-

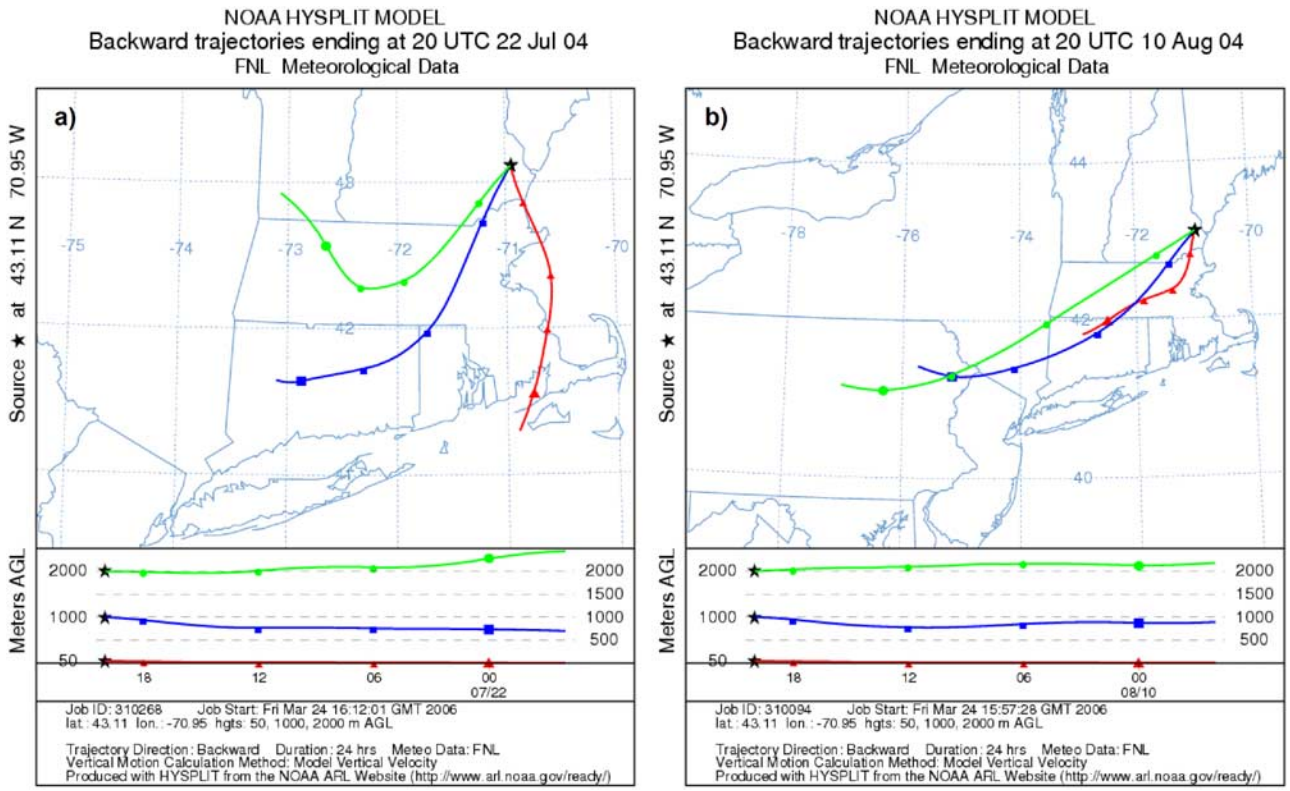

Figure 14. Selected back trajectories from ozone episodes with (a) high marine influences and (b) low marine influences.

sphere. At TF, air masses from the northeast and southeast had higher levels of $CHBr_3$ and CH_2Br_2 than those from the southwest and northwest. At AI, the highest average mixing ratios of $CHBr_3$ and CH_2Br_2 were observed when winds were from the northeast, southeast, and south–southwest (180–225°), which is indicative of the coastal marine influence. For C_2Cl_4 and C_2HCl_3, air masses from the southwest at TF and southwest–west (225–270°) at AI showed higher levels than those from other sectors, confirming a strong urban influence from these directions. Additionally, there were periods when air masses from the southeast (southeast–southwest at AI) showed a strong marine signature as well as enhancements of urban tracers, illustrating the complexity of the dynamic processes encountered in this region.

[49] At AI, $CHBr_3$ and CH_2Br_2 mixing ratios increased proportionally with wind speed, resulting from increased transfer to the atmosphere. The influence of Tropical Storm Bonnie was observed both at TF and AI, resulting in significant increases in mixing ratios of $CHBr_3$ and CH_2Br_2, as well as other marine tracers, during its passage through this region. The extended period of high winds in contact with supersaturated coastal waters during Tropical Storm Bonnie caused large amounts of halogenated compounds to be injected into the atmosphere, resulting in higher average mixing ratios at TF in summer 2004 as compared to previous years. Because tropical storms and hurricanes in the Atlantic Ocean regularly travel up the coastline during their transit northward, their presence may have profound effects on regions such as the northeastern United States.

[50] Marine tracers were used to investigate the transport and processing of polluted air masses along the northeast coastal region. At TF, O_3 episodes were identified during two meterological conditions, synoptic southwesterly and southeasterly onshore flow. Elevated O_3 levels corresponded to very low $CHBr_3$ mixing ratios during the southwesterly flow, suggesting a strong continental influence. Under the southeasterly onshore flow, enhanced levels of both O_3 and $CHBr_3$ were observed, indicating a pronounced marine influence. Ozone episodes related to air masses with strong marine influences accounted for 38% of all ozone episode days in the summers of 2003 and 2004 at TF.

[51] Coastal regions are potentially significant sources of short-lived brominated organic compounds to the atmosphere, with macroalgae playing an important role in their production. Meteorological conditions play a pivotal role in controlling the atmospheric abundances and distributions of these gases. It is not known how changes in wind speed via increased frequencies and strengths of tropical storms and hurricanes will alter the abundances and distributions of marine-derived gases in coastal regions, as sea-to-air fluxes are controlled by these factors. Long-term monitoring, including marine biomass investigations coupled with atmospheric and surface seawater measurements throughout the globe, is essential in order to have baseline measurements with which future changes can be compared.

[52] **Acknowledgments.** Financial support for this work was provided through the Office of Oceanic and Atmospheric Research at the National Oceanic and Atmospheric Administration under grants NA04OAR4600154

and NA05OAR4601080. Additional support for the research conducted on Appledore Island was provided by the National Science Foundation through grant 0401622. This paper is contribution number 148 to the Shoals Marine Laboratory. We thank the Shoals Marine Laboratory and the Isle of Shoals Steamship Company for their assistance and support during the field campaign. The authors gratefully acknowledge the NOAA Air Resources Laboratory (ARL) for the provision of the HYSPLIT transport and dispersion model and/or READY Web site (http://www.arl.noaa.gov/ready.html) used in this publication. Finally, we thank Daniel King from Drexel University for his constructive review of the manuscript, as well as Heather Allen from Ohio State University, Lissa Ducharme (UNH), and the UCI group.

References

Allonier, A. S., M. Khalanski, V. Camel, and A. Bermond (1999), Characterization of chlorination by-products in cooling effluents of coastal nuclear power stations, *Mar. Pollut. Bull.*, *38*(12), 1232–1241.

Atlas, E., S. M. Schauffler, J. T. Merrill, C. J. Hahn, B. Ridley, J. Walega, J. Greenberg, L. Heidt, and P. Zimmermann (1992), Alkyl nitrate and selected halocarbon measurements at Mauna Loa Observatory, Hawaii, *J. Geophys. Res.*, *97*, 10,331–10,348.

Blake, D. R., T.-Y. Chen, T. W. Smith Jr., C. J.-L. Wang, O. W. Wingenter, N. J. Blake, and F. S. Rowland (1996a), Three-dimensional distribution of nonmethane hydrocarbons and halocarbons over the northwestern Pacific during the 1991 Pacific Exploratory Mission (PEM-West A), *J. Geophys. Res.*, *101*, 1763–1778.

Blake, D. R., N. J. Blake, T. W. Smith Jr., O. W. Wingenter, and F. S. Rowland (1996b), Nonmethane hydrocarbon and halocarbon distributions during Atlantic Stratocumulus Transition Experiment/Marine Aerosol and Gas Exchange, June 1992, *J. Geophys. Res.*, *101*, 4501–4514.

Blake, N. J., et al. (1999a), Aircraft measurements of the latitudinal, vertical, and seasonal variations of NMHCs, methyl nitrate, methyl halides, and DMS during the First Aerosol Characterization Experiment (ACE 1), *J. Geophys. Res.*, *104*, 21,803–21,817.

Blake, N. J., et al. (1999b), Influence of Southern Hemispheric biomass burning on mid-tropospheric distributions of nonmethane hydrocarbons and selected halocarbons over the remote South Pacific, *J. Geophys. Res.*, *104*, 16,213–16,232.

Blake, N. J., et al. (2001), Large-scale latitudinal and vertical distributions of NMHCs and selected halocarbons in the troposphere over the Pacific Ocean during the March–April 1999 Pacific Exploratory Mission (PEM-Tropics B), *J. Geophys. Res.*, *106*, 32,627–32,644.

Blake, N. J., D. R. Blake, A. L. Swanson, E. Atlas, F. Flocke, and F. S. Rowland (2003), Latitudinal, vertical, and seasonal variations of C-1–C-4 alkyl nitrates in the troposphere over the Pacific Ocean during PEM-Tropics A and B: Oceanic and continental sources, *J. Geophys. Res.*, *108*(D2), 8242, doi:10.1029/2001JD001444.

Bottenheim, J. W., J. D. Fuentes, D. W. Tarasick, and K. G. Anlauf (2002), Ozone in the Arctic lower troposphere during winter and spring 2000 (ALERT 2000), *Atmos. Environ.*, *36*, 2535–2544.

Carpenter, L. J., and P. S. Liss (2000), On temperate sources of bromoform and other reactive organic bromine gases, *J. Geophys. Res.*, *105*, 20,539–20,547.

Carpenter, L. J., W. T. Sturges, S. A. Penkett, P. S. Liss, B. Alicke, K. Hebestreit, and U. Platt (1999), Short-lived alkyl iodides and bromides at Mace Head, Ireland: Links to biogenic sources and halogen oxide production, *J. Geophys. Res.*, *104*, 1679–1689.

Carpenter, L. J., P. S. Liss, and S. A. Penkett (2003), Marine organohalogens in the atmosphere over the Atlantic and Southern Oceans, *J. Geophys. Res.*, *108*(D9), 4256, doi:10.1029/2002JD002769.

Colman, J. J., A. L. Swanson, S. Meinardi, B. C. Sive, D. R. Blake, and F. S. Rowland (2001), Description of the analysis of a wide range of volatile organic compounds in whole air samples collected during PEM-Tropics A and B, *Anal. Chem.*, *73*(15), 3723–3731.

Dvortsov, V. L., M. A. Geller, S. Solomon, S. M. Schauffler, E. L. Atlas, and D. R. Blake (1999), Rethinking reactive halogen budgets in the midlatitude lower stratosphere, *Geophys. Res. Lett.*, *26*, 1699–1702.

Fischer, R. G., J. Kastler, and K. Ballschmiter (2000), Levels and pattern of alkyl nitrates, multifunctional alkyl nitrates, and halocarbons in the air over the Atlantic Ocean, *J. Geophys. Res.*, *105*, 14,473–14,494.

Fogelqvist, E., and M. Krysell (1991), Naturally and anthropogenically produced bromoform in the Kattegatt, a semi-enclosed oceanic basin, *J. Atmos. Chem.*, *13*, 315–324.

Foster, K. L., R. A. Plastridge, J. W. Bottenheim, P. B. Shepson, B. J. Finlayson-Pitts, and C. W. Spicer (2001), The role of Br_2 and BrCl in surface ozone destruction at polar sunrise, *Science*, *291*, 471–474.

Galbally, I. E., S. T. Bentley, and C. P. Meyer (2000), Mid-latitude marine boundary-layer ozone destruction at visible sunrise observed at Cape Grim, Tasmania, *Geophys. Res. Lett.*, *27*, 3841–3844.

Gschwend, P. M., J. K. Macfarlane, and K. A. Newman (1985), Volatile halogenated organic-compounds released to seawater from temperate marine macroalgae, *Science*, *227*, 1033–1035.

Jenner, H. A., C. J. L. Taylor, M. van Donk, and M. Khalanski (1997), Chlorination by-products in cooling water of some European coastal power stations, *Mar. Environ. Res.*, *43*, 279–293.

Keene, W. C., J. Stutz, A. P. Pszenny, J. R. Maben, E. Fischer, A. M. Smith, R. von Glasow, S. Pechtl, B. C. Sive, and R. K. Varner (2007), Inorganic chlorine and bromine in coastal New England air during summer, *J. Geophys. Res.*, *112*, D10S12, doi:10.1029/2006JD007689.

Liss, P. S., and L. Merlivat (1986), Air-sea gas exchange rates: Introduction and synthesis, in *The Role of Air-Sea Interactions in Geochemical Cycling*, edited by P. Buat-Menard, pp. 113–129, Springer, New York.

Manley, S. L., K. Goodwin, and W. J. North (1992), Laboratory production of bromoform, methylene bromide, and methyl iodide by macroalgae and distribution in near-shore southern California waters, *Limnol. Oceanogr.*, *37*(8), 1652–1659.

Mao, H., and R. Talbot (2004), Role of meteorological processes in two New England ozone episodes during summer 2001, *J. Geophys. Res.*, *109*, D20305, doi:10.1029/2004JD004850.

Mao, H., R. Talbot, C. Nielsen, and B. Sive (2006), Controls on methanol and acetone in marine and continental atmospheres, *Geophys. Res. Lett.*, *33*, L02803, doi:10.1029/2005GL024810.

McGivern, W. S., O. Sorkhabi, A. G. Suits, A. Deresckei-Kovacs, and S. W. North (2000), Primary and secondary processes in the photodissociation of $CHBr_3$, *J. Phys. Chem.*, *104*, 10,085–10,091.

Montzka, S. A., J. H. Butler, B. D. Hall, D. J. Mondeel, and J. W. Elkins (2003), A decline in tropospheric organic bromine, *Geophys. Res. Lett.*, *30*(15), 1826, doi:10.1029/2003GL017745.

Moody, J. L., J. W. Munger, A. H. Goldstein, D. J. Jacob, and S. C. Wofsy (1998), Harvard Forest regional-scale air mass composition by Patterns in Atmospheric Transport History (PATH), *J. Geophys. Res.*, *103*, 13,181–13,194.

Moore, R. M., and R. Tokarczyk (1993), Volatile biogenic halocarbons in the Northwest Atlantic, *Global Biogeochem. Cycles*, *7*, 195–210.

Nagao, I., K. Matsumoto, and H. Tanaka (1999), Sunrise ozone destruction found in the sub-tropical marine boundary layer, *Geophys. Res. Lett.*, *26*(22), 3377–3380.

Nielsen, J. E., and A. R. Douglass (2001), Simulation of bromoform's contribution to stratospheric bromine, *J. Geophys. Res.*, *106*, 8089–8100.

Nightingale, P. D., G. Malin, C. S. Law, A. J. Watson, P. S. Liss, M. I. Liddicoat, J. Boutin, and R. C. Upstill-Goddard (2000), In situ evaluation of air-sea gas exchange parameterizations using novel conservative and volatile tracers, *Global Biogeochem. Cycles*, *14*, 373–387.

Olaguer, E. P. (2002), The distribution of the chlorinated solvents dichloromethane, perchloroethylene, and trichloroethylene in the global atmosphere, *Environ. Sci. Pollut. Res.*, *9*, 175–182.

Pszenny, A. A. P., E. V. Fischer, R. S. Russo, B. C. Sive, and R. K. Varner (2007), Estimates of Cl atom concentrations and hydrocarbon kinetic reactivity in surface air at Appledore Island, Maine, during International Consortium for Atmospheric Research on Transport and Transformation/Chemistry of Halogens at the Isles of Shoals, *J. Geophys. Res.*, *112*, D10S13, doi:10.1029/2006JD007725.

Quack, B., and E. Suess (1999), Volatile halogenated hydrocarbons over the western Pacific between 43° and 4°N, *J. Geophys. Res.*, *104*, 1663–1678.

Quack, B., and D. W. R. Wallace (2003), Air-sea flux of bromoform: Controls, rates, and implications, *Global Biogeochem. Cycles*, *17*(1), 1023, doi:10.1029/2002GB001890.

Sander, R., and P. J. Crutzen (1996), Model study indicating halogen activation and ozone destruction in polluted air masses transported to the sea, *J. Geophys. Res.*, *101*, 9121–9138.

Schauffler, S. M., E. L. Atlas, D. R. Blake, F. Flocke, R. A. Lueb, J. M. Lee-Taylor, V. Stroud, and W. Travnicek (1999), Distributions of brominated organic compounds in the troposphere and lower stratosphere, *J. Geophys. Res.*, *104*, 21,513–21,535.

Schauffler, S. M., E. L. Atlas, S. G. Donnelly, A. Andrews, S. A. Montzka, J. W. Elkins, D. F. Hurst, P. A. Romashkin, G. S. Dutton, and V. Stroud (2003), Chlorine budget and partitioning during the Stratospheric Aerosol and Gas Experiment (SAGE) III Ozone Loss and Validation Experiment (SOLVE), *J. Geophys. Res.*, *108*(D5), 4173, doi:10.1029/2001JD002040.

Singh, H. B., A. N. Thakur, Y. E. Chen, and M. Kanakidou (1996), Tetrachloroethylene as an indicator of low Cl atom concentrations in the troposphere, *Geophys. Res. Lett.*, *23*, 1529–1532.

Sive, B. C. (1998), Atmospheric nonmethane hydrocarbons: Analytical methods and estimated hydroxyl radical concentrations, Ph.D. thesis, Univ. of Calif., Irvine.

Sive, B. C., Y. Zhou, D. Troop, Y. Li, W. C. Little, O. W. Wingenter, R. S. Russo, R. K. Varner, and R. Talbot (2005), Development of a

cryogen-free concentration system for measurements of volatile organic compounds, *Anal. Chem.*, *77*(21), 6989–6998, doi:10.1021/ac0506231.

Sturges, W. T., G. F. Cota, and P. T. Buckley (1992), Bromoform emission from Arctic ice algae, *Nature*, *358*(6388), 660–662.

Sturges, W. T., D. E. Oram, L. J. Carpenter, and S. A. Penkett (2000), Bromoform as a source of stratospheric bromine, *Geophys. Res. Lett.*, *27*, 2081–2084.

Swanson, A. L., N. J. Blake, E. Atlas, F. Flocke, D. R. Blake, and F. S. Rowland (2003), Seasonal variations of C_2–C_4 nonmethane hydrocarbons and C_1–C_4 alkyl nitrates at the Summit research station in Greenland, *J. Geophys. Res.*, *108*(D2), 4065, doi:10.1029/2001JD001445.

Varner, R. K., Y. Zhou, R. Russo, O. W. Wingenter, E. Atlas, C. Stroud, H. Mao, R. Talbot, and B. Sive (2008), Controls on atmospheric chloroiodomethane (CH_2C1I) in marine environments, *J. Geophys. Res.*, doi:10.1029/2007JD008889, in press.

von Glasow, R., R. Sander, A. Bott, and P. J. Crutzen (2002), Modeling halogen chemistry in the marine boundary layer: 1. Cloud-free MBL, *J. Geophys. Res.*, *107*(D17), 4341, doi:10.1029/2001JD000942.

Wang, C. J.-L. (1993), Global concentrations of selected halocarbons, 1988–1992, Ph.D. diss., Univ. of Calif., Irvine.

Wang, C. J.-L., D. R. Blake, and F. S. Rowland (1995), Seasonal variations in the atmospheric distribution of a reactive chlorine compound, tetrachloroethene ($CCl_2 = CCl_2$), *Geophys. Res. Lett.*, *22*, 1097–1100.

Wang, J.-L., C.-J. Chang, W.-D. Chang, C. Chew, and S.-W. Chen (1999), Construction and evaluation of automated gas chromatography for the measurement of anthropogenic halocarbons in the atmosphere, *J. Chromatogr. A*, *844*, 259–269.

Wanninkhof, R. (1992), Relationship between wind speed and gas exchange over the ocean, *J. Geophys. Res.*, *97*, 7373–7382.

Wingenter, O. W., M. K. Kubo, N. J. Blake, T. W. Smith Jr., D. R. Blake, and F. S. Rowland (1996), Hydrocarbon and halocarbon measurements as photochemical and dynamical indicators of atmospheric hydroxyl, atomic chlorine, and vertical mixing obtained during Lagrangian flights, *J. Geophys. Res.*, *101*, 4331–4340.

Wingenter, O. W., D. R. Blake, N. J. Blake, B. C. Sive, and F. S. Rowland (1999), Tropospheric hydroxyl and atomic chlorine concentrations, and mixing timescales determined from hydrocarbon and halocarbon measurements made over the Southern Ocean, *J. Geophys. Res.*, *104*, 21,819–21,828.

Wingenter, O. W., B. C. Sive, N. J. Blake, D. R. Blake, and F. S. Rowland (2005), Atomic chlorine concentrations derived from ethane and hydroxyl measurements over the equatorial Pacific Ocean: Implication for dimethyl sulfide and bromine monoxide, *J. Geophys. Res.*, *110*, D20308, doi:10.1029/2005JD005875.

World Meteorological Organization (2003), *Scientific Assessment of Ozone Depletion: 2002*, chap. 2, *Global Ozone Res. Monit. Proj. Rep. 47*, Geneva.

Yokouchi, Y., et al. (2005), Correlations and emission ratios among bromoform, dibromochloromethane, and dibromomethane in the atmosphere, *J. Geophys. Res.*, *110*, D23309, doi:10.1029/2005JD006303.

Zhou, Y. (2006), Atmospheric volatile organic compound measurements: Distributions and effects on air quality in coastal marine, rural and remote continental environments, Ph.D. thesis, Univ. of N. H., Durham.

Zhou, Y., R. K. Varner, R. S. Russo, O. W. Wingenter, K. B. Haase, R. Talbot, and B. C. Sive (2005), Coastal water source of short-lived halocarbons in New England, *J. Geophys. Res.*, *110*, D21302, doi:10.1029/2004JD005603.

J. Ambrose, H. Mao, R. S. Russo, B. C. Sive, R. Talbot, R. K. Varner, and Y. Zhou, Climate Change Research Center, Institute for the Study of Earth, Oceans and Space, University of New Hampshire, Durham, NH 03824, USA. (yzhou@ccrc.sr.unh.edu)

D. R. Blake, Department of Chemistry, University of California, Irvine, CA 92697, USA.

K. B. Haase and O. W. Wingenter, Department of Chemistry, New Mexico Tech, Socorro, NM 87801, USA.